Finite-Time Fault-Tolerant Attitude Stabilization for Spacecraft with Actuator Saturation

Qiang Shen, *Student Member, IEEE,* Danwei Wang, *Senior Member, IEEE,*
Senqiang Zhu, *Member, IEEE,* and Eng Kee Poh

Abstract

This paper addresses the finite-time fault-tolerant attitude stabilization control problem for a rigid spacecraft in the presence of actuator faults/failures, external disturbances, and modeling uncertainties. Firstly, a basic fault-tolerant controller is proposed to accommodate actuator faults/failures and guarantee local finite-time stability. When there is no a priori knowledge of actuator faults, disturbances, and inertia uncertainties, an on-line adaptive law is proposed to estimate the bounds of these uncertainties, and local finite-time convergence is achieved by an adaptive fault-tolerant controller. In addition, another adaptive fault-tolerant control scheme is derived which explicitly takes into account the actuator saturation. The proposed attitude controller provides fault-tolerant capability despite control input saturation and also ensures that attitude and angular velocity converge to a neighbourhood of the origin in finite time. Finally, simulation studies are presented to demonstrate the effectiveness of the proposed method.

Index Terms

Fault-tolerant control (FTC), finite-time convergence, actuator faults/failures, attitude stabilization, spacecraft.

I. Introduction

In safety-critical systems such as spacecrafts and aircrafts, reliability is particularly important as a minor fault in such systems can result in significant performance degradation or even instability. To enhance the system reliability and safety, a controller has to be capable of tolerating potential faults and maintaining desirable system performance. A way to ensure reliable operation of systems in the presence of undesirable faults is by means of fault-tolerant control (FTC) strategies [1]–[3], which can be classified into two categories, namely, passive FTC and active FTC. The active FTC approach reacts to the system component malfunctions by reconfiguring the controller based on real-time information from a fault detection and diagnosis (FDD) scheme. In contrast to active FTC approach, passive method utilizes a single robust controller to deal with all expected faults. Since neither FDD capability

The authors are with the School of Electrical and Electronic Engineering, Nanyang Technological University, Singapore 639798, Singapore (e-mail: qshen1@e.ntu.edu.sg; edwwang@ntu.edu.sg; sqzhu@ntu.edu.sg; eekpoh@ntu.edu.sg).

nor controller reconfiguration is required, the passive FTC approach is simpler to implement from a practical point of view. Furthermore, it has the advantage of avoiding time delay introduced by the online FDD and controller reconfiguration in active FTC. In practice, the fault can progress rapidly and the critical system may even become unstable before a desired active fault-tolerant controller can be synthesized [4], [5]. Motivated by the above, this paper focuses on the development of a passive fault-tolerant controller for a spacecraft attitude control system to handle actuator faults/failures.

There have been a great deal of results in the literature on spacecraft attitude control with actuator faults. For instance, in [6], based on feedback linearization control technique, a robust and asymptotically stable controller was implemented for automated attitude recovery of rigid and flexible spacecraft. In [7], an indirect robust adaptive FTC strategy for spacecraft attitude tracking was presented to accommodate actuator failures. With the use of a backstepping technique and three estimation filters, an adaptive FTC scheme was developed for spacecraft attitude stabilization in [8]. In [9], a velocity-free FTC feedback control law was proposed to solve the problem of fault tolerant attitude stabilization for a rigid spacecraft. In [10], a fault tolerant attitude tracking controller based on variable structure approach was proposed for attitude control of spacecraft, where the transient response of the closed-loop system was controlled by suitable choice of a dedicated parameter.

Although all the above-mentioned FTC approaches can accommodate actuator faults, most of them only guarantee asymptotic stability, which means that the system states converge to the equilibrium as time tends to infinity. For some spacecraft missions, such as remote sensing or reconnaissance, the spacecraft is required to achieve rapid attitude maneuvering together with high targeting accuracy and stability between the maneuvers [11]. Thus, finite-time convergence in [12] becomes applicable, as it ensures fast convergence, high precision control performance, and better disturbance rejection [12], [13]. It should be pointed out that the authors of [14] present some results on finite time stability concerning the transient behavior of a system response, which is different from that defined in [12]. In [15], fast terminal sliding mode (FTSM) control schemes were used for spacecraft attitude control to achieve finite time convergence. In [16], a finite-time attitude coordination control scheme for spacecraft formation flying was derived on the basis of modified FTSM. Based on geometric homogeneity technique, two simple proportional-derivative controllers are proposed for finite-time stabilization of spacecraft in [17] to achieve fast transient and high-precision performance. However, these controllers are designed without considering actuator faults, and so they are unsuitable for FTC of the spacecraft attitude control system. Recently, in [18], a finite-time fault-tolerant controller was proposed for spacecraft attitude tracking system to accommodate two types of reaction wheel fault.

Another key issue that should be addressed in spacecraft attitude control systems as well as FTC systems is actuator saturation. Due to the physical limitations of the actuator, it may not be able to generate typically commanded control torque. Particularly, in the event of actuator faults/failures, the remaining actuators are required to generate higher torques to compensate for the faulty actuators to maintain system performance [19]–[22]. As a result, actuator faults/failures may potentially lead to saturation of the actuators, which will lead to further damage to the rest of the system or even instability of the closed-loop system if there is no appropriate control strategy to dump the saturated actuators [19], [22]. A number of spacecraft attitude control schemes which handle actuator

saturation can be found in [23]–[26] and the reference therein. It should be pointed out that control allocation is an effective way to solve the actuator saturation problem when redundant actuators are available [27], [28]. In the case of actuator faults/failures, since on-line information on the effectiveness of the actuators is required in control allocation precess, an FDD scheme is necessary (see, for example, [29]–[31], and [32]). However, whatever FDD method is employed, the estimate of fault information will not be perfect [32]. As a result, control allocation algorithm may not be able to realize the desired control effect, especially when actuator saturation limits are present [33]. In addition, most of the aforementioned control allocation strategies are proposed and implemented in an open-loop manner [34], [35], as the stability of such closed-loop system under using control allocation with the baseline controller could not be guaranteed theoretically [36].

This paper investigates the FTC problem for spacecraft attitude stabilization, where local finite-time stability or ultimate boundedness of the closed-loop trajectories is achieved with explicit regard to actuator faults and control input saturation. In order to achieve finite-time stability, FTSM manifold is introduced. Assuming that there exists a priori knowledge of faults and uncertain system parameters, a basic finite-time fault-tolerant controller is proposed to accommodate four types of actuator faults/failures in the presence of bounded external disturbances and inertia uncertainties. Furthermore, with the aid of adaptation mechanism, two adaptive FTC approach is proposed, which can ensure locally finite-time convergence in both the reaching phase and the sliding phase despite actuator faults/failures. The main contributions of this paper are stated as follows:

1) With consideration of the actuator redundancy, four types of common reaction wheel faults/failures are accommodated by the proposed fault-tolerant controllers.
2) Based on fast terminal sliding mode control technique, local finite-time stability for spacecraft attitude maneuver in the presence of the external disturbances, inertia uncertainties, actuator faults/failures, can be guaranteed by the use of Lyapunov direct approach.
3) The proposed final adaptive finite-time fault-tolerant controller not only has the capability to protect the actuator from saturation, but also guarantees that attitude and angular velocity converge to a neighbourhood of the origin in finite time without FDD scheme under actuator faults/failures.

The remaining part of the paper is organized as follows. In Section II, the mathematical models for the rigid spacecraft and actuator fault are introduced. The design and analysis of a basic finite-time fault-tolerant controller and two adaptive finite-time FTC schemes are addressed in Section III. To verify the effectiveness of the proposed fault-tolerant controllers, the simulation studies are given in Section IV, followed by conclusions in Section V.

II. PRELIMINARIES

A. Spacecraft Dynamic Equation and Kinematics Equation

The spacecraft is modeled as a rigid body with reaction wheel as actuators. The nonlinear differential equations that govern the kinematics and dynamics of the spacecraft in terms of quaternion can be expressed as [28], [37]

$$J(\cdot)\dot{\omega} = -\omega\times (J(\cdot)\omega + DJ_w\Omega) + D\tau + d(t) \tag{1}$$

$$\dot{q}_v = \frac{1}{2}(q_v \times \omega + q_0\omega) \tag{2}$$

$$\dot{q}_0 = -\frac{1}{2}{q_v}^T\omega, \tag{3}$$

where $J(\cdot) \in \mathbb{R}^{3\times 3}$ is the inertia matrix of the spacecraft, $\omega \in \mathbb{R}^3$ is the angular velocity vector of the spacecraft with respect to an inertial frame $\mathcal{I}$ and expressed in the body frame $\mathcal{B}$, $Q = [q_0, q_1, q_2, q_3]^T = [q_0, q_v^T]^T \in \mathbb{R}\times\mathbb{R}^3$ denotes the unit quaternion describing the attitude orientation of the body frame $\mathcal{B}$ with respect to inertial frame $\mathcal{I}$ and satisfies the constraint $q_0^2 + q_v^T q_v = 1$, $\tau \in \mathbb{R}^n (n > 3)$ is the control torque produced by n reaction wheels, $J_w = diag\left([J_{w1}, J_{w2}, \ldots, J_{wn}]\right) \in \mathbb{R}^{n\times n}$ is the inertia matrix of reaction wheels, $\Omega \in \mathbb{R}^n$ is the angular velocity of the reaction wheel, $D \in \mathbb{R}^{3\times n}$ is the reaction wheel distribution matrix, $d(t) \in \mathbb{R}^3$ is the external disturbance. Note that the symbol $\times$ denotes the vector cross product. The control torques τ generated by the reaction wheel are given by

$$\tau = -J_w\dot{\Omega}. \tag{4}$$

Here, it is assumed that there exists uncertainty in the matrix $J(\cdot)$, i.e. $J(\cdot) = J_0 + \Delta J$, where J_0 and ΔJ denote the nominal part and uncertain part of $J(\cdot)$, respectively. Then (1) can be rewritten as

$$J_0\dot{\omega} = -\omega\times J_0\omega - \omega\times DJ_w\Omega + D\tau + d(t) - \Delta J\dot{\omega} - \omega^\times \Delta J\omega. \tag{5}$$

Property 1: The nominal part J_0 of inertia matrix is a symmetric and positive definite matrix and can be lower and upper bounded as follows:

$$J_1\|x\|^2 \le x^T J_0 x \le J_2\|x\|^2, \qquad \forall x \in \mathbb{R}^3 \tag{6}$$

where J_1 and J_2 are some positive constants, and $\|\cdot\|$ denotes Euclidean norm of vectors and largest singular value for matrices.

B. Actuator Faults/Failures Model

The actuator considered in this paper is reaction wheel, which consists of a flywheel and an electric motor. When the rotation speed of the flywheel is changed, the spacecraft begins to counter-rotate proportionately through conservation of angular momentum. A fault/failure may occur in several components of the reaction wheel, such as faulty electronics, drive motor, and power supply, etc. As discussed in [38], [39], reaction wheels are sensitive devices that are vulnerable to the following four main sources of faults/failures:

1) *Decreased reaction torque* (**F1**): Due to increased friction between stator and rotor, inadequate lubrication and marginal failures in bearings, and decreased motor torque, the rate of change of the wheel speed might be less than the nominal value. As a consequence, the generated reaction wheel output torque could be less than the commanded torque by the controller.
2) *Increased bias torque* (**F2**): Because of changes in coulomb friction and viscous friction of the bearings caused by aging, time-varying temperature, and lubrication, the wheel may not be capable of holding its speed, which may accelerate or decelerate the wheel gradually. Therefore, a low bias torque is produced even when the commanded attitude control toque is zero.
3) *Failure to respond to control signals* (**F3**): If malfunction occurs in drive electronics, drive motor, and power supply, the reaction wheel may decelerate slowly or hold its speed, without any response to control signals.
4) *Continuous generation of reaction torque* (**F4**): Faults in the bus voltage and intermittent time-varying faults in the motor current might lead to continuous increase or decrease in wheel speed, thereby generating reaction torque, independent of the commanded torque by the controller.

Based on the definitions of fault and failure from [40], **F1** and **F2** could be categorized as actuator fault, while **F3** and **F4** could be categorized as actuator failure. When a fault occurs in one reaction wheel, the reaction wheel is still usable but may have a slower response or become less effective. But once a failure occurs, the reaction wheel may undergo a catastrophic or complete breakdown, which is much more severe than a fault. If one of the reaction wheel experiences **F3**-**F4**, actuator redundancy should be used to ensure three-axis control of the attitude control system and maintain performance. On the other hand, the above four types of reaction wheel faults/failures can also be classified on the basis of their effects on the output behaviour of the reaction wheel, and **F1**-**F4** of the reaction wheel can be described as partial loss of effectiveness fault, bias fault, outage failure, and hardover failure, respectively.

The above four types of reaction wheel faults/failures can be mathematically modelled as

$$\tau_i = e_i(t)u_{ci} + \bar{u}_i, \tag{7}$$

where u_{ci} denotes the desired torque signal of the ith reaction wheel generated by the controller with $i = 1, 2, \ldots, n$, $0 \leq e_i(t) \leq 1$ represents the effectiveness factor of the ith reaction wheel, $\bar{u}_i$ is the uncertain faulty input entering the spacecraft in an additive way, and τ_i denotes the actual control action exerted on the spacecraft. In the situation of fault-free, the actual output torque of an actuator is equal to its desired value, i.e., $\tau_i = u_{ci}$, with $e_i(t) = 1$ and $\bar{u}_i = 0$. Corresponding relations between model parameters and reaction wheel faults/failure are summarized in Table I.

According to (7), the actual control torque τ generated by n reaction wheels can be written as follows:

$$\tau = E(t)u_c + \bar{u}, \tag{8}$$

where $u_c = [u_{c1}, u_{c1}, \ldots, u_{cn}]^T \in \mathbb{R}^n$ denotes the input torque vector of the n actuators, $E(t) = diag([e_1(t), e_2(t), \ldots, e_n(t)]) \in \mathbb{R}^{n\times n}$ represents the actuator control effectiveness matrix, and $\bar{u} = [\bar{u}_1, \bar{u}_2, \ldots, \bar{u}_n]^T \in \mathbb{R}^n$ is the

TABLE I
RELATIONS BETWEEN MODEL PARAMETERS AND REACTION WHEEL FAULTS/FAILURES

Fault/Failure	Type	e_i	$\bar{u}_i$
F1	Partial loss of effectiveness fault	$0 < e_i < 1$	0
F2	Bias fault	1	$\bar{u}_i \neq 0$
F3	Outage failure	0	0
F4	Hardover failure	0	$\bar{u}_i \neq 0$

additive actuator fault vector. Hence, the attitude dynamic model with reaction wheel faults/failures **F1**-**F4** can be written as

$$J_0\dot{\omega} = -\omega\times J_0\omega - \omega\times DJ_w\Omega + DE(t)u_c + D\bar{u} + d(t) - \Delta J\dot{\omega} - \omega\times\Delta J\omega. \tag{9}$$

C. Transformed Spacecraft Attitude Dynamics

To express the attitude dynamics in a more convenient manner for controller design, the Lagrange-like equation is adopted to describe spacecraft attitude dynamics. Denoting $T = \frac{1}{2}[R(q_v) + q_0 I_3] \in \mathbb{R}^{3\times 3}$, where $R(x)$ is a skew-symmetric matrix for $x, y \in \mathbb{R}^3$ such that $x \times y = R(x)y$. Then, equation (2) can be expressed as

$$\omega = P\dot{q}_v, \tag{10}$$

with

$$P = T^{-1} = \left[\frac{1}{2}(R(q_v) + q_0 I_3)\right]^{-1}. \tag{11}$$

After taking the time derivative of (10), the following expression for $\dot{\omega}$ is obtained:

$$\dot{\omega} = \dot{P}\dot{q}_v + P\ddot{q}_v. \tag{12}$$

Substituting (10) and (12) into (9) and premultiplying both sides of the resulting expression by P^T lead to

$$J^*\ddot{q}_v = -\Xi\dot{q}_v + P^T(DJ_w\Omega)\times P\dot{q}_v + P^T DE(t)u_c + P^T D\bar{u} + T_d, \tag{13}$$

where $J^* = P^T J_0 P$, $\Xi = P^T J_0 \dot{P} - P^T(J_0 P\dot{q}_v)\times P$, and $T_d = P^T(d(t) - \Delta J\dot{\omega} - \omega\times\Delta J\omega)$. Here, T_d is considered as the lumped disturbances and uncertainties. Regarding the dynamic model given in (13) and Property 1, the following properties are given according to [41].

Property 2: The inertia matrix J^* is symmetric positive definite, and the matrix $\dot{J}^* - 2\Xi$ satisfies the following skew-symmetric relationship:

$$x^T\left(\dot{J}^* - 2\Xi\right)x = 0. \qquad \forall x \in \mathbb{R}^3 \tag{14}$$

Property 3: The inertia matrix J^* is lower and upper bounded, and satisfies the following bounded condition:

$$\underline{J}\|x\|^2 \leq x^T J^* x \leq \bar{J}\|x\|^2, \qquad \forall x \in \mathbb{R}^3 \tag{15}$$

where $\underline{J}$ and $\bar{J}$ are positive constants.

For the development of control law, the following assumptions are given.

Assumption 1: To ensure that P defined in (11) exists, the following condition should be satisfied [41]:

$$det(T) = \frac{1}{2}q_0 \neq 0. \qquad \forall t \in [0, \infty) \tag{16}$$

In order to guarantee that (16) remains valid, it is required that the initial value of q_0 satisfy this constraint, and that the subsequent controller is designed to guarantee that $q_0 \neq 0$ for all $t > 0$.

Assumption 2: The external disturbance d in (1) is upper bounded by a constant, and the lumped term T_d of the disturbances and uncertainties satisfies the following condition [42]:

$$\|T_d\| \leq \gamma_0 \Phi, \tag{17}$$

where $\Phi = 1 + \|\omega\| + \|\omega\|^2$, and γ_0 is a positive constant.

Assumption 3: The additive fault introduced in the fault model (8) satisfies

$$\|\bar{u}\| \leq f_0, \tag{18}$$

where f_0 is a positive constant.

Assumption 4: The positive definite matrix DED^T satisfies

$$0 < e_0 \leq \min\{\lambda_{min}(DED^T), 1\}, \tag{19}$$

where $\lambda_{min}(\cdot)$ represents the minimum eigenvalue of a matrix and e_0 is a positive constant.

Remark 1: The model of the lumped variable T_d in assumption 2 can be generalized to $\|T_d\| \leq \gamma_0 + \gamma_{01}\|\omega\| + \gamma_{02}\|\omega\|^2$ to reduce the conservativeness, where γ_{01} and γ_{02} are two constants. However, two additional design parameters are introduced, which will complicate the design process and increase the computational complexity, especially to the case of adaptive fault-tolerant controller design. The assumption 4 means that, although the n actuators $(n > 3)$ may suffer from partial loss of actuator effectiveness or even complete failure, the number of totally failed actuators is no more than $n-3$ such that DED^T remains positive definite. If more than $n-3$ actuators have totally failed, the matrix DED^T becomes singular and the system is underactuated. In such a situation, other types of actuator have to be employed [37]. The underactuated system is not considered further in this paper.

D. FTSM Manifold Design

To develop the control scheme, the FTSM manifold $s \in \mathbb{R}^3$ is defined as

$$s = \dot{q}_v + \alpha q_v + \beta sig\,(q_v)^r = 0, \tag{20}$$

where α and β are positive constants, $r = \frac{r_1}{r_2}$, r_1 and r_2 are positive odd integers and $0 < r < 1$, and the function $sig(x)^r$ is defined as

$$sig(x)^r = [|x_1|^r sign(x_1),\, |x_2|^r sign(x_2),\, |x_3|^r sign(x_3)]^T$$

where x_j is the jth component of $x \in \mathbb{R}^3$, $j = 1, 2, 3$.

Differentiating sliding function s with respect to time yields

$$\dot{s} = \ddot{q}_v + \alpha \dot{q}_v + \beta r \, diag(|q_v|^{r-1}) \dot{q}_v. \tag{21}$$

Since (21) contains a negative fractional power $r-1$, the singularity will occur if $q_{vj} = 0$ and $\dot{q}_{vj} \neq 0$. To avoid singularity, first order derivative of s is modified as [43]

$$\dot{s} = \ddot{q}_v + \alpha \dot{q}_v + \beta q_{vr}, \tag{22}$$

with $q_{vr} \in \mathbb{R}^3$ defined as

$$q_{vr,j} = \begin{cases} r|q_{vj}|^{r-1}\dot{q}_{vj}, & if \, |q_{vj}| \geq \epsilon, \, and \, \dot{q}_{vj} \neq 0 \\ r|\epsilon|^{r-1}\dot{q}_{vj}, & if \, |q_{vj}| < \epsilon, \, and \, \dot{q}_{vj} \neq 0 \\ 0, & \dot{q}_{vj} = 0 \end{cases} \tag{23}$$

where $q_{vr,j}$ is the jth component of q_{vr}, ϵ is a small positive constant. Then, considering (13), (20), and (22), it can be shown that

$$J^* \dot{s} = -\Xi s + P^T D E u_c + P^T D \bar{u} + P^T (D J_w \Omega) \times P \dot{q}_v + \Xi \alpha q_v + \Xi \beta sig(q_v)^r + J^* \alpha \dot{q}_v + J^* \beta q_{vr} + T_d. \tag{24}$$

The above equation can be further simplified as

$$J^* \dot{s} = -\Xi s + P^T D E u_c + P^T D \bar{u} + F + T_d, \tag{25}$$

where $F = P^T (D J_w \Omega) \times P \dot{q}_v + \Xi \alpha q_v + \Xi \beta sig(q_v)^r + J^* \alpha \dot{q}_v + J^* \beta q_{vr}$.

The following results will be used in Sec. III to derive finite-time stability proof for the proposed controller design.

Lemma 1 [15]: Suppose $a_1, a_2, \ldots, a_n$ are positive numbers and $0 < p < 2$, then the following inequality holds:

$$(a_1^2 + a_2^2 + \cdots + a_n^2)^p \leq (a_1^p + a_2^p + \cdots + a_n^p)^2. \tag{26}$$

Lemma 2 [12]: Suppose $V(x)$ is a continuous positive-definite function (defined on $\mathcal{D} \in \mathbb{R}$) and $\dot{V}(x) + \lambda V^\rho(x)$ is negative semi-definite on $\in \mathbb{R}$ for $0 < \rho < 1$ and $\lambda > 0$, then there exist an area $\mathcal{D}_0 \in \mathbb{R}$ such that any $V(x)$ which starts from $\mathcal{D}_0 \in \mathbb{R}$ can reach $V(x) \equiv 0$ in finite time. Moreover, if T_{reach} is the time needed to reach $V(x) \equiv 0$, then

$$T_{reach} \leq \frac{V^{1-\rho}(x_0)}{\lambda(1-\rho)}, \tag{27}$$

where $V(x_0)$ is the initial value of $V(x)$.

Lemma 3 [44]: Assume $\rho_1 > 0$, $\rho_2 > 0$, and $0 < \rho < 1$, if a continuous positive definite function V satisfies the following inequality:

$$\dot{V} \leq -\rho_1 V - \rho_2 V^\rho, \qquad \forall t > 0 \tag{28}$$

then, it can be found that V which starts from $V(x_0)$ can reach $V \equiv 0$ in finite time. Moreover, the reaching time T_{reach} is given by

$$T_{reach} \leq \frac{1}{\rho_1(1-\rho)} \ln \frac{\rho_1 V^{1-\rho}(0) + \rho_2}{\rho_2}. \tag{29}$$

Lemma 4: Consider the terminal sliding mode manifold s defined by (20). If the sliding mode manifold satisfies $s = 0$, then the system states q_v and $\dot{q}_v$ are globally finite-time stable, i.e., the system states q_v and $\dot{q}_v$ which start from $q_v(0)$ and $\dot{q}_v(0)$ will converge to $q_v = 0$ and $\dot{q}_v = 0$ in finite time, respectively.

Proof. See the Appendix A. □

III. Fault-Tolerant Controller Design

In this section, we shall show the development of an adaptive finite-time fault-tolerant controller to solve the attitude stabilization problem under actuator faults/failues (**F1**-**F4**) and control input saturation. Three control schemes are proposed. Firstly, a basic finite-time fault tolerant controller is designed assuming a priori knowledge of the bounds on disturbances, uncertainties, and actuator faults/failures is known. Subsequently, an adaptive finite-time fault-tolerant controller is designed without relying on any prior knowledge. Finally, the results are extended to the case in which actuator saturation is considered.

A. Basic Finite-Time Fault-Tolerant Controller Design

For the attitude dynamics defined in (25) with actuator faults/failures, assuming parameters γ_0, f_0, and e_0, which respectively represent the upper bounds on the lumped disturbances and uncertainties, upper bound of additive fault and lower bound of the minimum eigenvalue of DED^T, are known, the basic finite-time FTC law is designed as

$$u_c = -D^T P \left[u_{nom} + (\gamma_1 \|D\| + \gamma_2 \|P\| \|u_{nom}\|) \frac{s}{\|Ps\|} \right], \tag{30}$$

with

$$u_{nom} = \frac{k\|s_\rho\|_1 + (\|F\| + \gamma_0 \Phi)\|s\|}{\|Ps\|^2} s, \tag{31}$$

where k is a positive scalar, s_ρ is a column vector defined as $s_\rho = [s_1^{\rho+1}, s_2^{\rho+1}, s_3^{\rho+1}]^T$, ρ is a positive scalar satisfying $0 < \rho < 1$, γ_1 and γ_2 are positive scalars satisfying $\gamma_1 = \frac{f_0+\varepsilon}{e_0}$ and $\gamma_2 = \frac{1-e_0+\varepsilon}{e_0}$ respectively with ε is a small positive scalar.

Theorem 1: Consider the attitude control systems described by (1-3) in the presence of four types of reaction wheel faults/failures **F1**-**F4**. If Assumptions 1-4 are satisfied and the controller (30) is applied, then the closed-loop system will be locally stabilized in finite time, i.e., $q_v \to 0$, $\omega \to 0$ in finite time.

Proof. See the Appendix B. □

Remark 2: Since finite-time stability requires that system states converge to the equilibrium in finite time, finite-time stability is therefore a much stronger requirement than asymptotic stability [45], whose convergence rate is at best exponential. Hence, the closed-loop systems under finite-time controller will have a faster convergence rate

[12], [13]. Moreover, the convergence time for achieving attitude stabilization can be given by Lemma 2 and Lemma 3.

Remark 3: It should be pointed out that $q_v \to 0$, $\omega \to 0$ in finite time is proved here, and the state q_0 is not considered. When $q_v = 0$, it is obtained that $q_0 = \pm 1$ from the constraint condition on unit quaternion. Therefore, there exist two equilibrium points, i.e., $Q = [1, 0, 0, 0]^T$ and $Q = [-1, 0, 0, 0]^T$. However, due to the fact that both equilibrium points correspond to a unique physical equilibrium orientation [46], it is only needed to guarantee that $q_v \to 0$ in finite time. In addition, due to the Assumption 1 that requires $q_0(t) \neq 0$ for all $t \geq 0$, local finite-time stability is obtained in Theorem 1, as well as the following two theorems in Sec. III.B and Sec. III.C. In order to remove this assumption and get global result, some switching method nay be incorporated into the controller design, such as [47], but this is not within the scope investigated in this work.

Remark 4: Note that for the fault-free case with all actuators functional, finite-time stability can also be guaranteed by choosing the same control scheme in (30). This is easily shown by applying the same procedure outlined in the proof of Theorem 1, which implies that the proposed controller in (30) is able to achieve attitude stabilization in finite time irrespective of whether actuator faults occur or not.

B. Adaptive Finite-Time Fault-Tolerant Controller Design

In the first basic finite-time FTC law, the bounds on the inertia uncertainties, external disturbances and actuator faults/failures are assumed to be known to the designer in advance. In practice, these information on the bounds are not always available due to the complicated structure of disturbance, time-varying inertia property, and unexpected characteristics of faults/failures. Therefore, in order to avoid the requirements of a priori knowledge of these bounds, an adaptive mechanism is introduced to estimate these bounds information.

The adaptive finite-time FTC law is designed as

$$u_c = -D^T P \left[u_{nom} + (\hat{\gamma}_1 \|D\| + \hat{\gamma}_2 \|P\| \|u_{nom}\|) \frac{s}{\|Ps\|} \right], \tag{32}$$

with

$$u_{nom} = \frac{(k + \|F\| + \hat{\gamma}_0 \Phi)\|s\|}{\|Ps\|^2} s, \tag{33}$$

where k is a positive scalar, $\hat{\gamma}_0$, $\hat{\gamma}_1$, and $\hat{\gamma}_2$ are the estimated values of γ_0, $\gamma_1 = \frac{f_0+\varepsilon}{e_0}$, and $\gamma_2 = \frac{1-e_0+\varepsilon}{e_0}$, respectively. The adaptive laws are chosen as

$$\dot{\hat{\gamma}}_0 = c_0(\Phi\|s\| - \delta_0 \hat{\gamma}_0), \tag{34a}$$

$$\dot{\hat{\gamma}}_1 = c_1(\|D\|\|Ps\| - \delta_1 \hat{\gamma}_1), \tag{34b}$$

$$\dot{\hat{\gamma}}_2 = c_2(\|P\|\|u_{nom}\|\|Ps\| - \delta_2 \hat{\gamma}_2), \tag{34c}$$

where $c_i > 0$ and $\delta_i > 0$ $(i = 0, 1, 2)$ are the design parameters, and the initial estimated values satisfy $\hat{\gamma}_i(0) > 0$.

Lemma 5 [48]: Given the parameter adaptive law in (34a)-(34c), the parameters γ_i as well as their estimates $\hat{\gamma}_i$ have upper bounds, i.e., there always exist positive scalars $\bar{\gamma}_i$ such that $\hat{\gamma}_i \leq \bar{\gamma}_i$ and $\gamma_i \leq \bar{\gamma}_i$ for all $t > 0$, respectively.

Theorem 2: Consider the attitude control systems described by (1-3) in the presence of four types of reaction wheel faults/failures **F1**-**F4**. If the adaptive controller (32) and update laws in (34a-34c) are applied under Assumptions 1-4, the sliding mode manifold will converge to the neighborhood of $s = 0$ as

$$\|s\| \leq \Delta_s \tag{35}$$

in finite time, where $\Delta_s = \sqrt{\frac{2}{\underline{j}}}\frac{\phi}{\delta}$, δ and ϕ are positive scalars to be defined later. Furthermore, the spacecraft attitude q_{vj} and angular velocity ω_j $(j = 1, 2, 3)$ will locally converge to the regions

$$|q_{vj}| \leq \min\left\{\frac{|\Delta_s|}{\alpha}, \left(\frac{|\Delta_s|}{\beta}\right)^{\frac{1}{r}}\right\}, \quad |\omega_j| \leq 6\sqrt{3}\Delta_s \tag{36}$$

in finite time, respectively.

Proof. See the Appendix C. □

Remark 5: It should be noted that, the control scheme in (32) is independent of the parameters e_0 and f_0. Thus, there is no need to involve a FDD block to identify actuator faults and the proposed fault-tolerant controller is able to accommodate actuator faults/failures automatically and adaptively whenever actuator faults/failures occur.

Remark 6: As can be seen from (35), the accuracy of the sliding manifold is related to the parameters δ and ϕ. Specifically, the larger the parameter δ or the smaller the parameter ϕ is, the smaller Δ_s becomes. Also, it is clear in (36) that the final accuracy of attitude stabilization is related to the parameters α, β, and r. Thus, it can be concluded that larger α and β and a smaller r lead to better performance.

C. Adaptive Finite-Time Fault-Tolerant Controller with Input Saturation

To deal with input saturation problem, the adaptive finite-time fault-tolerant controller from Theorem 2 is further enhanced with explicit consideration of actuator saturation. If actuator saturation is taken into consideration, assume that all n actuator control torques are constrained by a common saturation value, given by

$$|u_{ci}| \leq u_{\max}, \tag{37}$$

where $u_{\max}$ is a positive constant representing the maximum allowable control torque and $i = 1, \ldots, n$. The following input saturation function is taken into consideration:

$$u_c^{sat} = \mathcal{X}(u_c)\, u_c, \tag{38}$$

where $\mathcal{X}(u_c) = diag\left(\mathcal{X}_1(u_{c1}), \mathcal{X}_2(u_{c2}), \ldots, \mathcal{X}_n(u_{cn})\right)$, with

$$\mathcal{X}_i(u_{ci}) = \begin{cases} \frac{u_{\max}}{u_{ci}} sign(u_{c,i}), & \text{if } |u_{ci}| > u_{\max} \\ 1, & \text{if } |u_{ci}| \leq u_{\max} \end{cases}. \tag{39}$$

Therefore, the dynamics of spacecraft defined in (25) can be written as

$$J^* \dot{s} = -\Xi s + P^T D E u_c^{sat} + P^T D \bar{u} + F + T_d. \tag{40}$$

Since $0 < \min_i \left(\mathcal{X}_i \left(u_c(t)\right)\right) \leq 1$, according to the density property of real number [49], [50], there always exists a constant κ such that

$$0 < \kappa \leq \min_i \left(\mathcal{X}_i \left(u_c(t)\right)\right) \leq 1, \qquad \forall u_c(t),\, t \in [0, \infty)\,. \tag{41}$$

Now, the adaptive fault-tolerant control law ensuring attitude stabilization under actuator fault and control input saturation is proposed as

$$u_c = -D^T P \left[u_{nom} + \zeta \hat{\theta}_3 \left(\hat{\theta}_1 \|D\| + \hat{\theta}_2 \|P\| \|u_{nom}\|\right) \frac{s}{\|Ps\|}\right], \tag{42}$$

with

$$u_{nom} = \frac{(k + \|F\| + \hat{\theta}_0 \Phi)\|s\|}{\|Ps\|^2}\, s. \tag{43}$$

where k is a positive scalar, $\hat{\theta}_0$, $\hat{\theta}_1$, $\hat{\theta}_2$, and $\hat{\theta}_3$ denote the estimations of constants $\theta_0 = \gamma_0$, $\theta_1 = \frac{f_0+\varepsilon}{e_0}$, and $\theta_2 = \frac{1-e_0\kappa+\varepsilon}{e_0}$, and $\theta_3 = \kappa^{-1}$, respectively. The adaptive laws are chosen as

$$\dot{\hat{\theta}}_0 = c_0(\Phi\|s\| - \delta_0 \hat{\theta}_0), \tag{44a}$$

$$\dot{\hat{\theta}}_1 = c_1(\|D\|\|Ps\| - \delta_1 \hat{\theta}_1), \tag{44b}$$

$$\dot{\hat{\theta}}_2 = c_2(\|P\|\|u_{nom}\|\|Ps\| - \delta_2 \hat{\theta}_2), \tag{44c}$$

$$\dot{\hat{\theta}}_3 = \text{Proj}_{\hat{\theta}_3} \left\{c_3 \zeta \hat{\theta}_3^3 \left[\left(\hat{\theta}_1 \|D\| + \hat{\theta}_2 \|P\| \|u_{nom}\|\right) \|Ps\| - \delta_3 \hat{\theta}_3\right]\right\}, \tag{44d}$$

where $\zeta > 1$, $c_i > 0$ and $\delta_i > 0$ $(i = 0, 1, \ldots, 3)$ are the design parameters, and the initial estimated values satisfy $\hat{\theta}_0(0) > 0$, $\hat{\theta}_1(0) > 0$, $\hat{\theta}_2(0) > 0$, and $\hat{\theta}_3(0) \geq 1$, respectively. $\text{Proj}_{\hat{\theta}_3}(\bullet)$ denotes the projection operator defined as

$$\text{Proj}_{\hat{\theta}_3}(\bullet) = \begin{cases} \bullet, & \text{if } \hat{\theta}_3 > 1 \\ \bullet, & \text{if } \hat{\theta}_3 = 1 \text{ and } \bullet \geq 0 \\ 0, & \text{if } \hat{\theta}_3 = 1 \text{ and } \bullet < 0 \end{cases}$$

whose role is to keep the estimate $\hat{\theta}_3$ within the interval $[1, +\infty)$ because of the physical meaning of κ.

Lemma 6 [48]: Given the parameter adaptive law in (44a)-(44d), the parameters θ_i as well as their estimates $\hat{\theta}_i$ have upper bounds, i.e., there always exist positive scalars $\bar{\theta}_i$ such that $\hat{\theta}_i \leq \bar{\theta}_i$ and $\theta_i \leq \bar{\theta}_i$, $i = 0, 1, \ldots, 3$, for all $t > 0$, respectively.

Theorem 3: Consider the attitude control systems described by (1-3) with control input saturation in the presence of four types of reaction wheel faults/failures **F1**-**F4**. If the adaptive controller (42) and update laws (44a-44d) are applied under Assumptions 1-4, the sliding mode manifold will locally converge to the neighborhood of $s = 0$ as

$$\|s\| \leq \Delta_{sat} \tag{45}$$

in finite time, where $\Delta_{sat} = \sqrt{\frac{2}{J}} \frac{\varphi}{\eta}$, and φ and η and are two positive scalars to be defined later. Furthermore, the spacecraft attitude $q_{v,j}$ and angular velocity ω_j $(j = 1, 2, 3)$ will converge to the region

$$|q_{vj}| \leq \min\left\{\frac{\Delta_{sat}}{\alpha}, \left(\frac{\Delta_{sat}}{\beta}\right)^{\frac{1}{r}}\right\}, \quad |\omega_j| \leq 6\sqrt{3}\Delta_{sat} \tag{46}$$

in finite time, respectively.

Proof. See the Appendix D. □

Remark 7: The saturated adaptive fault-tolerant controller in Theorem 3 is also applicable when the actuator is fault-free but with actuator saturation constraint. Since the fault-free case ($e_i(t) = 1$ and $\bar{u}_i = 0$) is also included in the controller design of Theorem 3, by following the same procedure outlined in the proof of Theorem 3, it is guaranteed that attitude and angular velocity converge to a neighbourhood of the origin in finite time with explicit consideration of the actuator saturation no matter actuator faults/failures occur or not.

Remark 8: The proposed control law is discontinuous due to the functions $\frac{s}{\|Ps\|}$ and $\frac{s}{\|Ps\|^2}$, which may lead to undesirable phenomenon of chattering in the sliding mode. This problem can be alleviated by replacing the discontinuous functions $\frac{s}{\|Ps\|}$ and $\frac{s}{\|Ps\|^2}$ by continuous functions $\frac{s}{\|Ps\|+\xi}$ and $\frac{s}{\|Ps\|^2+\xi}$, respectively, where ξ is a small positive scalar [51].

IV. Numerical Examples and Simulations

To demonstrate the effectiveness and performance of the proposed controller, simulation results are presented in this section. Consider the spacecraft model given in (1-3) with four reaction wheels in a pyramid configuration with the actuator distribution matrix D given in [37]. The moment inertia of each reaction wheel is $J_w = 0.015 I_4$ kg·m^2.

The nominal inertia matrix of the spacecraft is $J_0 = diag([140, 120, 130])$ kg·m^2. Due to energy consumption and onboard payload deployment, the uncertainty in the inertia matrix ΔJ is considered, which is the same as in [7]. The initial attitude orientation is chosen as $q_v(0) = [0.3, -0.3, 0.2]^T$ and $q_0(0) = \sqrt{1 - q_v^T q_v}$. The initial angular velocity of the spacecraft is $\omega(0) = [0, 0, 0]^T$ rad/s. The initial angular velocity of reaction wheel is set as $\Omega(0) = [50, 50, 50, 50]^T$ rad/s. The external disturbance model is in the form of $d(t) = 0.005 \times [\sin(0.8t), \cos(0.5t), \cos(0.3t)]^T$ N·m. The parameters in FTSM manifold defined in (20) are chosen as $\alpha = 0.05$, $\beta = 0.01$, $r_1 = 3$, and $r_2 = 5$. In order to accomplish critical mission, the spacecraft must provide high attitude pointing accuracy and stability of the pointing such that $|q_{vj}| \leq 1.0 \times 10^{-4}$ and $|\omega_j| \leq 5.0 \times 10^{-5}$, $j = 1, 2, 3$.

A. Basic Finite-Time Fault-Tolerant Controller

In this section, the actuator fault scenario is described as follows. The first reaction wheel experiences an increased bias torque **F2** (bias fault) with a negative additive bias torque $\bar{u}_1 = -(0.06\sin(0.8t) + 0.04)$ N·m after 50 s and the second reaction wheel decreases 50% of its normal actuation torque **F1** (partial loss of effectiveness fault) after 5 s. The third reaction wheel loses 60% of its effectiveness in the time interval from 5 s to 60 s, and further experiences an additive bias fault with a negative bias torque $\bar{u}_3 = -(0.02\sin(0.3t) + 0.02)$ N·m after 60 s. The fourth reaction wheel fails to respond to control signals **F3** (outage) after 10 s. The model of bias fault can be found in [52].

For the purpose of comparison, the proposed basic finite-time fault-tolerant control (BFT-FTC) scheme in (30) and the traditional proportional-derivative control (PDC) scheme [28] are compared under the aforementioned reaction

wheel faults. To make a fair comparison of the control performances (e.g., strong robustness and convergence rate), the magnitude of control torques under two control schemes are limited to the same level. The performances of attitude quaternion, angular velocity as well as command control inputs using the BFT-FTC scheme and the PDC method are presented in Figs. 1-3, respectively. From Figs. 1a and 2a, the attitude control requirements for the mission are met by using the BFT-FTC scheme despite external disturbances, inertia uncertainties, and actuator faults. In contrast, the attitude control system with PDC scheme cannot accomplish the mission due to the reaction wheel faults/failures. The control performance comparison of the BFT-FTC scheme and the PDC scheme is shown in Table II in terms of settling time and steady-state precision. As shown in Table II, the BFT-FTC scheme performs significantly better than the PDC scheme with higher steady precision and shorter settling time in both attitude and angular velocity response. The commanded reaction wheel control torque under the two schemes are depicted in Fig. 3. These simulation results show that not only good attitude stabilization performance but also fault tolerance capability can be obtained with the proposed BFT-FTC scheme.

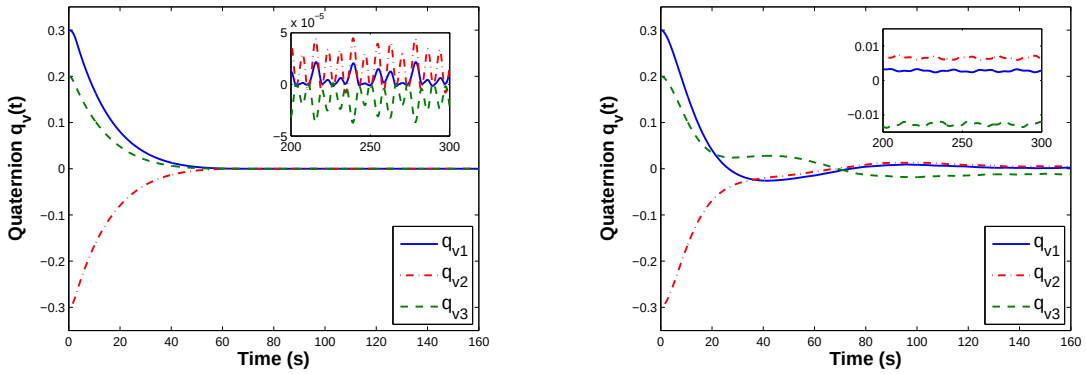

(a) BFT-FTC (b) PDC

Fig. 1. Spacecraft attitude response under BFT-FTC scheme and PDC scheme.

TABLE II

COMPARISON OF CONTROL PERFORMANCE BETWEEN BFT-FTC SCHEME AND PDC SCHEME

Control scheme	Control performance			
	Settling time of q_v (s)	Steady precision of q_v	Settling time of ω (s)	Steady precision of ω
BFT-FTC	68	5.0×10^{-5}	70	4.5×10^{-5}
PDC	120	1.5×10^{-2}	135	8.0×10^{-4}

B. Adaptive Finite-Time Fault-Tolerant Controller

To illustrate the effectiveness of the proposed adaptive finite-time fault-tolerant control (AFT-FTC) scheme defined in (32), the attitude stabilization problem under actuator faults/failures in the absence of a priori knowledge of

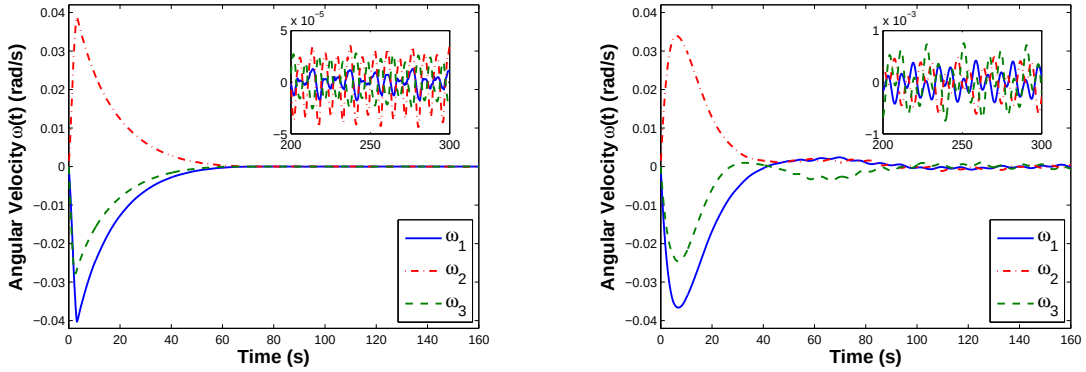

(a) BFT-FTC (b) PDC

Fig. 2. Spacecraft angular velocity response under BFT-FTC scheme and PDC scheme.

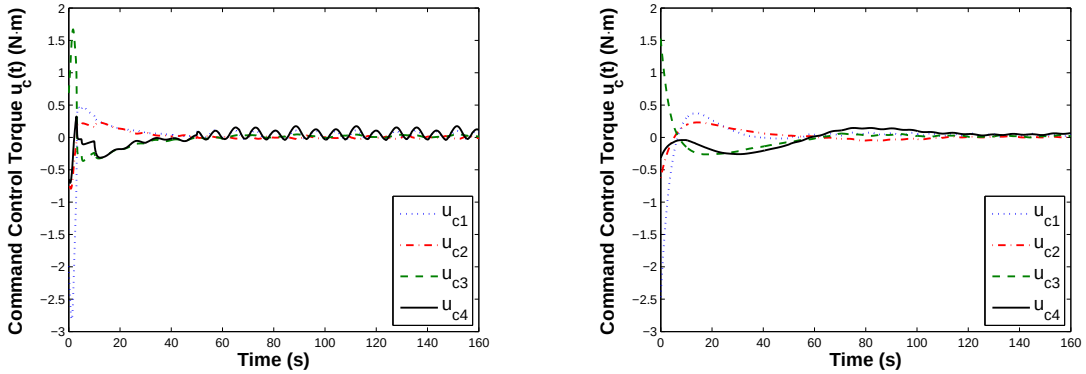

(a) BFT-FTC (b) PDC

Fig. 3. Commanded control torque under BFT-FTC scheme and PDC scheme.

system parameters is simulated in this section. For comparison purpose, the indirect robust adaptive fault-tolerant control (IRA-FTC) method presented in [7] is also simulated. In the simulation, the reaction wheels are assumed to experience the same fault scenario as described in Sec. IV.A. All the controller parameters of AFT-FTC scheme in (32) are identical to those used in the BTF-FTC scheme in Sec IV.A, and the corresponding parameters of the adaptation law defined in (34a-34c) are chosen with $c_0 = 0.1$, $c_1 = 1$, $c_2 = 1$, $\delta_0 = 0.02$, $\delta_1 = 0.002$, and $\delta_2 = 0.001$. The initial values of $\hat{\gamma}_0$, $\hat{\gamma}_1$, and $\hat{\gamma}_2$ are selected as $\hat{\gamma}_0(0) = 0.005$, $\hat{\gamma}_1(0) = 0.1$, and $\hat{\gamma}_2(0) = 0.1$, respectively. To smooth the proposed fault-tolerant controller, the parameter ξ in Remark 8 is chosen as 0.0002. Similarly, in order to properly evaluate the performance and allow fair comparison between the AFT-FTC and IRA-FTC scheme, the magnitude of control torques under two controllers are limited to the same level.

The attitude quaternion and spacecraft angular velocity are shown in Figs. 4 and 5. The results show that both the AFT-FTC scheme and the IRA-FTC scheme can stabilize the attitude quaternion and angular velocity to a

neighborhood of zero in spite of inertia uncertainties, time-varying disturbances, and reaction wheel faults. As shown by the steady-state behavior in Figs. 4 and 5, the attitude pointing accuracy and the stabilization accuracy under the AFT-FTC scheme are 4.0×10^{-5} and 3.5×10^{-5}, respectively. Thus, the mission can be successfully accomplished by the AFT-FTC scheme. In contrast, the IRA-FTC scheme cannot meet the attitude control requirements for the mission when the control torques are at the same level as under the AFT-FTC scheme. The control performance comparison of the BFT-FTC scheme and the IRA-FTC scheme is shown in Table III. By comparing the performance of the two schemes, it is clear that the AFT-FTC can achieve better attitude pointing accuracy and faster convergence rate than that of the IRA-FTC scheme. The commanded reaction wheel control torques of the two schemes are shown in Fig. 6. Referring to Fig. 7, it is observed that the adaptive parameters $\hat{\gamma}_0$, $\hat{\gamma}_1$, and $\hat{\gamma}_2$ are bounded, and thus the efficacy of the proposed adaptation laws in (34a)-(34c) are verified. These simulation results show that fairly good control performance is achieved by the proposed AFT-FTC approach even under such severe reaction wheel faults and unknown uncertainty bounds which are required to be known in the BFT-FTC scheme.

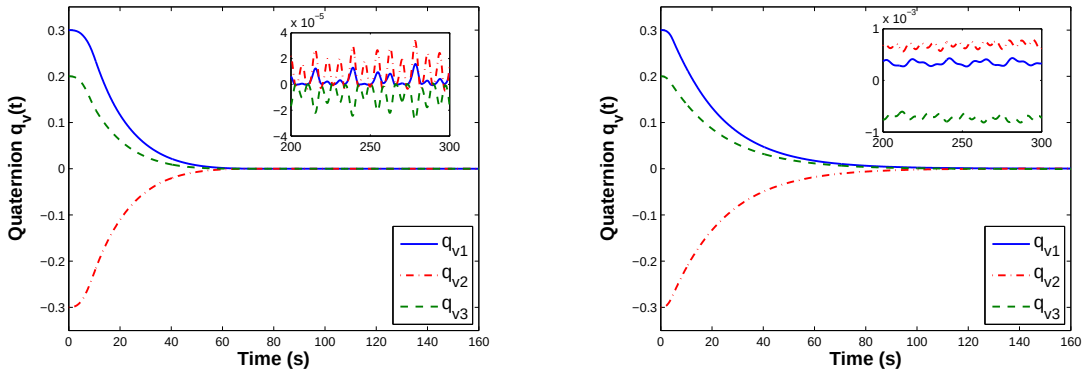

(a) AFT-FTC (b) IRA-FTC

Fig. 4. Spacecraft attitude under AFT-FTC scheme and IRA-FTC scheme.

TABLE III

COMPARISON OF CONTROL PERFORMANCE BETWEEN AFT-FTC SCHEME AND IRA-FTC SCHEME

Control scheme	Control performance			
	Settling time of q_v (s)	Steady precision of q_v	Settling time of ω (s)	Steady precision of ω
AFT-FTC	73	4.0×10^{-5}	72	3.5×10^{-5}
IRA-FTC	128	8.0×10^{-4}	138	1.5×10^{-4}

C. Adaptive Finite-Time Fault-Tolerant Controller with Actuator Saturation

In this subsection, besides reaction wheel faults/failures, control input saturation is also simulated. For comparison study, the saturated version of IRA-FTC (SIRA-FTC) scheme in [7] and the AFT-FTC scheme with actuator

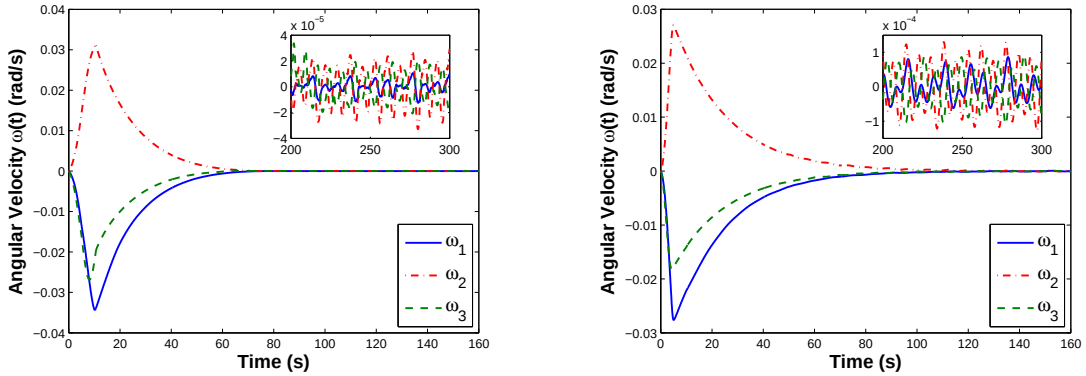

(a) AFT-FTC (b) IRA-FTC

Fig. 5. Spacecraft angular velocity response under AFT-FTC scheme and IRA-FTC scheme.

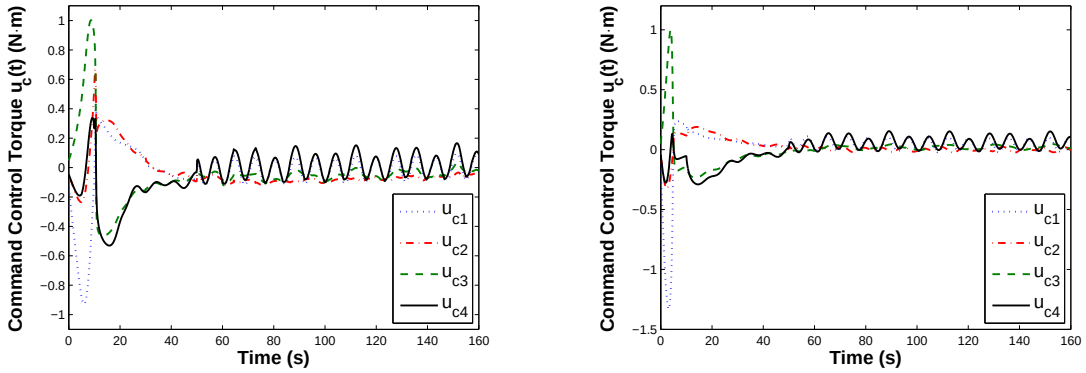

(a) AFT-FTC (b) IRA-FTC

Fig. 6. Commanded control torque under AFT-FTC scheme and IRA-FTC scheme.

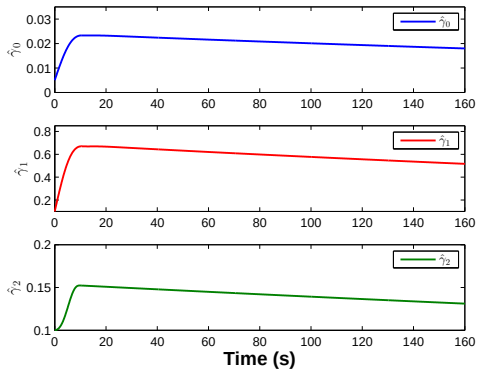

Fig. 7. Time response of adaptive parameters $\hat{\gamma}_0(t)$, $\hat{\gamma}_1(t)$, and $\hat{\gamma}_2(t)$ under AFT-FTC scheme.

saturation (SAFT-FTC) designed in (42) are investigated. The maximum torque of each reaction wheel for both two control schemes is constrained to be 0.2 N·m, i.e., $u_{max} = 0.2$ N·m. The reaction wheel fault scenario is the same as presented in Sec. IV.A except the bias faults are changed to be $\bar{u}_1 = -(0.012\sin(0.8t) + 0.008)$ N·m for the first reaction wheel and $\bar{u}_3 = -(0.004\sin(0.8t) + 0.004)$ N·m for the third one, respectively. The control gains for the SAFT-FTC scheme are chosen as $\zeta = 1.5$, $c_0 = 0.1$, $c_1 = 1$, $c_2 = 1$, $c_3 = 0.1$, $\delta_0 = 0.02$, $\delta_1 = 0.001$, $\delta_2 = 0.001$, and $\delta_3 = 0.01$. The initial values of $\hat{\theta}_0$, $\hat{\theta}_1$, $\hat{\theta}_2$, and $\hat{\theta}_3$ are chosen to be $\hat{\theta}_0(0) = 0.005$, $\hat{\theta}_1(0) = 0.1$, $\hat{\theta}_2(0) = 0.1$, and $\hat{\theta}_3(0) = 1$, respectively. In order to smooth the proposed SAFT-FTC scheme, the parameter ξ in Remark 8 is chosen as 0.004. The other design parameters remain unchanged from those used in the previous AFT-FTC scheme.

From Figs. 8a and 9a, it can be observed that the attitude and the angular velocity under the SAFT-FTC scheme converge to the neighborhood of zero in finite time despite actuator faults and control input saturation limits, and that satisfactory stabilization error and a good convergency can be achieved. However, due to the effects of control input saturation, the convergence rate of attitude in Fig. 8a is slower than the situation without input saturation as shown in Fig. 4a. This phenomena is often referred to as graceful degradation in performance [19]. As shown in Fig. 10a, it is clearly seen that the commanded control input is always within the maximum magnitude of the reaction wheel. Figs. 8b, 9b, and 10b show attitude quaternion, angular velocity, and command control input when the SIRA-FTC scheme is applied. The control performance comparison of the SAFT-FTC scheme and the SIRA-FTC scheme is shown in Table IV. Although the SIRA-FTC scheme can stabilize the spacecraft attitude to a certain level, the attitude pointing accuracy is lower than that of the SAFT-FTC scheme and doesn't meet the mission performance requirements. In addition, similar to the previous simulation case, the proposed SAFT-FTC scheme can provide faster convergence rate than the SIRA-FTC scheme. The bounded adaptive parameters $\hat{\theta}_0$, $\hat{\theta}_1$, $\hat{\theta}_2$, and $\hat{\theta}_3$ are shown in Fig. 11. Moreover, referring to Fig. 10, it is interesting to see that actuator saturation constraints can be satisfied by both fault-tolerant controllers. However, the allowed control torque ($u_{max} = 0.2$ N·m) under the SIRA-FTC scheme is not fully used, which can be observed from Fig. 10b, where the actual maximal control toque is only about 0.15 N·m. Hence, the SIRA-FTC method in [7] is much more conservative than the proposed SAFT-FTC scheme.

TABLE IV

COMPARISON OF CONTROL PERFORMANCE BETWEEN SAFT-FTC SCHEME AND SIRA-FTC SCHEME

Control scheme	Control performance			
	Settling time of q_v (s)	Steady precision of q_v	Settling time of ω (s)	Steady precision of ω
SAFT-FTC	82	3.5×10^{-5}	83	4.0×10^{-5}
SIRA-FTC	183	4.0×10^{-4}	160	4.0×10^{-5}

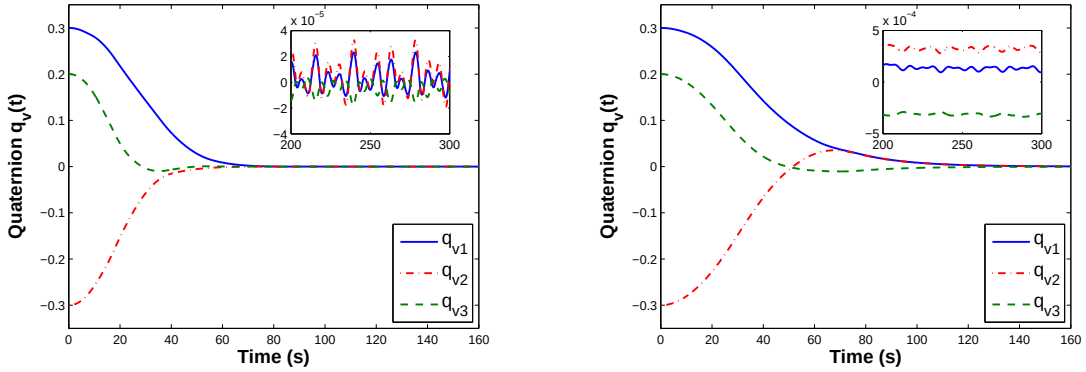

(a) SAFT-FTC (b) SIRA-FTC

Fig. 8. Spacecraft attitude under SAFT-FTC scheme and SIRA-FTC scheme.

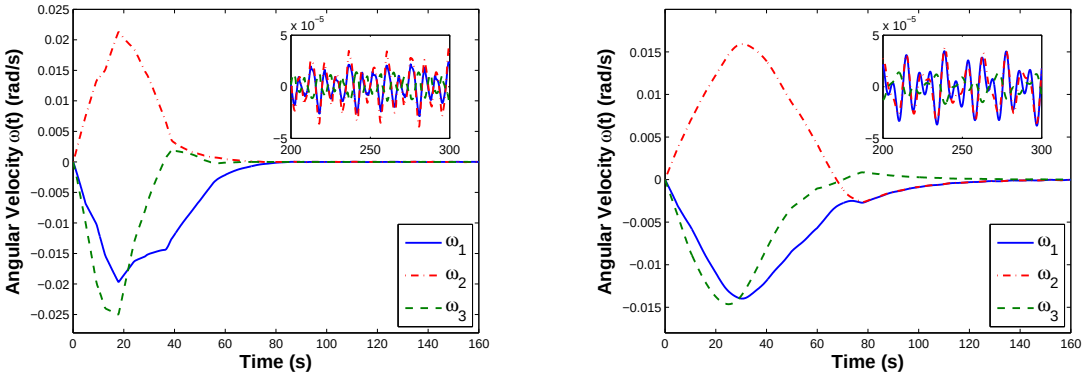

(a) SAFT-FTC (b) SIRA-FTC

Fig. 9. Spacecraft angular velocity response under SAFT-FTC scheme and SIRA-FTC scheme.

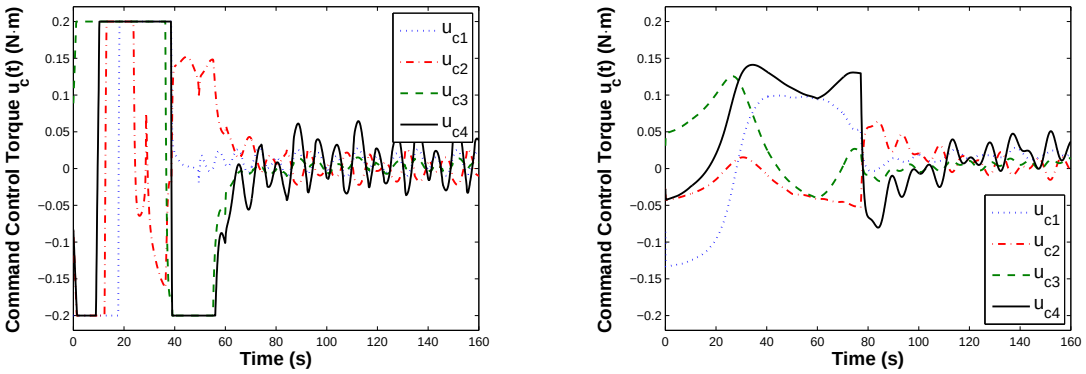

(a) SAFT-FTC (b) SIRA-FTC

Fig. 10. Commanded control torque under SAFT-FTC scheme and SIRA-FTC scheme.

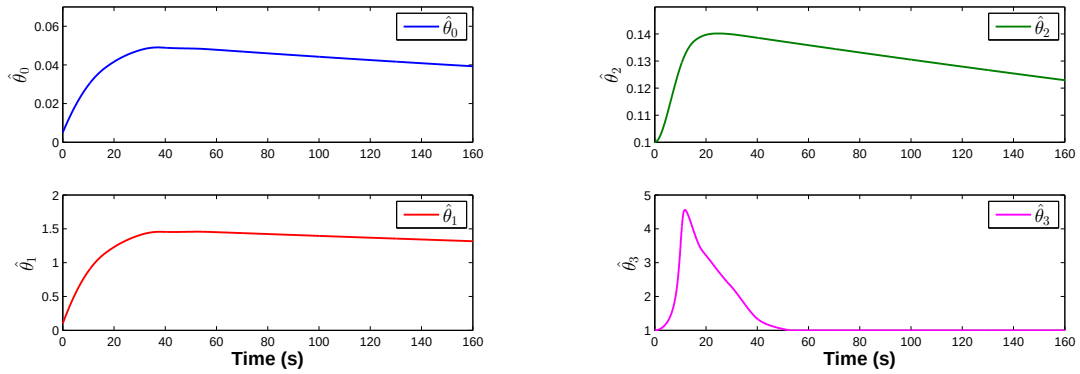

(a) $\hat{\theta}_0(t)$ and $\hat{\theta}_1(t)$ under SAFT-FTC scheme

(b) $\hat{\theta}_2(t)$ and $\hat{\theta}_3(t)$ under SAFT-FTC scheme

Fig. 11. Time response of adaptive parameters $\hat{\theta}_0(t)$, $\hat{\theta}_1(t)$, $\hat{\theta}_2(t)$, and $\hat{\theta}_3(t)$ under SAFT-FTC scheme.

V. Conclusions

In this paper, adaptive finite-time FTC scheme has been investigated for rigid spacecraft subject to uncertainties in inertia matrix, four types of actuator faults/failures as well as actuator saturation. Firstly, based on the terminal sliding mode theory, a basic finite-time fault-tolerant controller has been proposed. Then, incorporating the adaptive strategy, an adaptive finite-time fault-tolerant controller is developed. The proposed adaptive controller is effective against actuator faults/failures and also guarantees finite-time convergence without requiring any a priori knowledge of fault and uncertainty information. In addition, the adaptive fault-tolerant controller is further enhanced to address control input constraints. The Lyapunov direct approach is employed to prove the local stability of the closed-loop system and to show the finite-time convergence of the system states. Finally, simulation studies have been presented to illustrate the effectiveness of the proposed finite-time FTC schemes.

Further research is needed to address the problem of global finite-time stabilization of spacecraft subject to actuator faults/failures and actuator saturation. Moreover, since the estimate of the upper bound information on spacecraft uncertainties, disturbances, and magnitude of faults/failures is used to design the controller, the proposed controller may turn out to be conservative from performance perspective. To reduce such conservativeness, active FTC can be carried out, where a FDD scheme is used to provide timely and accurate fault information and a reconfigured controller is synthesized to compensate the effects of the fault/failure. Experimental study including designing testbed and testing the proposed approach is also important from an application point of view.

Appendix A

Proof of Lemma 4. In order to prove that q_v can converge to $q_v = 0$ in finite time after the sliding mode manifold $s = 0$ is achieved, a candidate Lyapunov function is constructed as follows:

$$V_0 = \frac{1}{2} q_v^T q_v. \tag{47}$$

Taking the time derivative of the Lyapunov function (47) alone sliding mode manifold $s = 0$ yields

$$\dot{V}_0 = q_v^T \left[-\alpha q_v - \beta sig(q_v)^r\right] \leq -\varrho_1 V_0 - \varrho_2 V_0^{\varsigma}, \tag{48}$$

where $\varrho_1 = 2\alpha$, $\varrho_2 = 2^{\frac{r+1}{2}}\beta$, $\varsigma = \frac{r+1}{2}$, and Lemma 1 is applied. It is clear that (48) has a similar structure to (28), and therefore, using Lemma 3, it can be concluded that q_v converges to origin in finite time. Furthermore, because the sliding manifold $s = 0$ is guaranteed, $\dot{q}_v$ will also converge to the origin along the sliding manifold in finite time. This completes the proof. □

APPENDIX B

Proof of Theorem 1. Consider the following Lyapunov function candidate

$$V_1 = \frac{1}{2} s^T J^* s. \tag{49}$$

Using (25), the time derivative of V_1 is

$$\begin{aligned}\dot{V}_1 &= \frac{1}{2} s^T \dot{J}^* s + s^T J^* \dot{s} \\ &= \frac{1}{2} s^T \dot{J}^* s + s^T \left(-\Xi s + P^T D E u_c + P^T D \bar{u} + F + T_d\right).\end{aligned}$$

In view of the control law (30) and Property 2, it follows that

$$\begin{aligned}\dot{V}_1 \leq\ & s^T P^T (I_3 - DED^T) P u_{nom} - s^T P^T P u_{nom} - (\gamma_1 \|D\| + \gamma_2 \|P\| \|u_{nom}\|) \frac{s^T P^T D E D^T P s}{\|Ps\|} \\ & + f_0 \|D\| \|Ps\| + \|F\| \|s\| + \|T_d\| \|s\| \\ \leq\ & (1 - e_0) \|P\| \|u_{nom}\| \|Ps\| - e_0 \gamma_1 \|D\| \|Ps\| - s^T P^T P \frac{k \|s_\rho\|_1 + (\|F\| + \gamma_0 \Phi) \|s\|}{\|Ps\|^2} s + \|F\| \|s\| \\ & - e_0 \gamma_2 \|P\| \|u_{nom}\| \|Ps\| + f_0 \|D\| \|Ps\| + \|T_d\| \|s\| \\ \leq\ & -k \sum_{j=1}^{3} |s_j|^{\rho+1} + (1 - e_0 - e_0\gamma_2) \|p\| \|u_{nom}\| \|Ps\| + (f_0 - e_0\gamma_1) \|D\| \|Ps\| + (\|T_d\| - \gamma_0 \Omega) \|s\|. \end{aligned} \tag{50}$$

With the definition of γ_1 and γ_2, and by using Assumption 2, it can be shown that

$$\dot{V}_1 \leq -k \sum_{j=1}^{3} |s_j|^{\rho+1}. \tag{51}$$

From Property 3 and Lemma 1, the following inequalities can be obtained:

$$\dot{V}_1 \leq -k \left(\frac{2}{\bar{J}}\right)^{\frac{\rho+1}{2}} \left(\sum_{j=1}^{3} \frac{\bar{J}}{2} s_j^2\right)^{\frac{\rho+1}{2}} \leq -K V_1^{\frac{\rho+1}{2}}, \tag{52}$$

where $K = k \left(\frac{2}{\bar{J}}\right)^{\frac{\rho+1}{2}} > 0$. According to Lemma 2, because K is a positive scalar, and $0 < \frac{\rho+1}{2} < 1$, the sliding manifold will reach $s = 0$ in finite time. Furthermore, from Lemma 4, $q_v = 0$ is achieved in finite time as well as $\dot{q}_v$ will converge to origin. Then, according to (2) and Assumption 1, it can be concluded that $\omega = 0$ is also achieved in finite time. This completes the proof. □

APPENDIX C

Proof of Theorem 2. Consider the following Lyapunov function candidate V_2:

$$V_2 = \frac{1}{2}s^T J^* s + \frac{1}{2c_0}(\hat{\gamma}_0 - \bar{\gamma}_0)^2 + \frac{e_0}{2c_1}(\hat{\gamma}_1 - \bar{\gamma}_1)^2 + \frac{e_0}{2c_2}(\hat{\gamma}_2 - \bar{\gamma}_2)^2. \tag{53}$$

Taking the time derivative of V_2 and using (25), the control law (32), and Property 2, it leads to

$$\begin{aligned}\dot{V}_2 \leq\ & (1-e_0)\|P\|\|u_{nom}\|\|Ps\| - s^T P^T P u_{nom} - e_0\hat{\gamma}_1\|D\|\|Ps\| - e_0\hat{\gamma}_2\|P\|\|u_{nom}\|\|Ps\| \\ & + f_0\|D\|\|Ps\| + \|F\|\|s\| + \|T_d\|\|s\| + \frac{1}{c_0}(\hat{\gamma}_0 - \bar{\gamma}_0)\dot{\hat{\gamma}}_0 + \frac{e_0}{c_1}(\hat{\gamma}_1 - \bar{\gamma}_1)\dot{\hat{\gamma}}_1 + \frac{e_0}{c_2}(\hat{\gamma}_2 - \bar{\gamma}_2)\dot{\hat{\gamma}}_2. \end{aligned} \tag{54}$$

Applying adaptive laws (34a-34c) and u_{nom} defined in (33), the following inequalities can be obtained:

$$\begin{aligned}\dot{V}_2 \leq & -k\|s\| + (\gamma_0 - \bar{\gamma}_0)\Phi\|s\| + (f_0 - e_0\bar{\gamma}_1)\|D\|\|Ps\| + (1 - e_0 - e_0\bar{\gamma}_2)\|P\|\|u_{nom}\|\|Ps\| \\ & - \delta_0(\hat{\gamma}_0 - \bar{\gamma}_0)\hat{\gamma}_0 - e_0\delta_1(\hat{\gamma}_1 - \bar{\gamma}_1)\hat{\gamma}_1 - e_0\delta_2(\hat{\gamma}_2 - \bar{\gamma}_2)\hat{\gamma}_2. \end{aligned} \tag{55}$$

Using the following facts by completion of squares:

$$-(\hat{\gamma}_i - \bar{\gamma}_i)\hat{\gamma}_i \leq -\left(\hat{\gamma}_i - \frac{\bar{\gamma}_i}{2}\right)^2 + \frac{\bar{\gamma}_i^2}{4}, \tag{56}$$

where $i = 0, 1, 2$, we have

$$\begin{aligned}\dot{V}_2 \leq & -k\|s\| - \delta_0\left[\left(\hat{\gamma}_0 - \frac{\bar{\gamma}_0}{2}\right)^2 - \frac{\bar{\gamma}_0^2}{4}\right] - e_0\delta_1\left[\left(\hat{\gamma}_1 - \frac{\bar{\gamma}_1}{2}\right)^2 - \frac{\bar{\gamma}_1^2}{4}\right] - e_0\delta_2\left[\left(\hat{\gamma}_2 - \frac{\bar{\gamma}_2}{2}\right)^2 - \frac{\bar{\gamma}_2^2}{4}\right] \\ = & -k\|s\| - \delta_0|\hat{\gamma}_0 - \bar{\gamma}_0| - e_0\delta_1|\hat{\gamma}_1 - \bar{\gamma}_1| - e_0\delta_2|\hat{\gamma}_2 - \bar{\gamma}_2| \\ & + \delta_0\left(|\hat{\gamma}_0 - \bar{\gamma}_0| + \frac{\bar{\gamma}_0^2}{4}\right) + e_0\delta_1\left(|\hat{\gamma}_1 - \bar{\gamma}_1| + \frac{\bar{\gamma}_1^2}{4}\right) + e_0\delta_2\left(|\hat{\gamma}_2 - \bar{\gamma}_2| + \frac{\bar{\gamma}_2^2}{4}\right). \end{aligned} \tag{57}$$

With the help of Lemma 1, Lemma 5, and Property 3, it can be found that

$$\dot{V}_2 \leq -\delta V_2^{\frac{1}{2}} + \phi, \tag{58}$$

where δ and ϕ are positive scalars defined by $\delta = \min\left\{k\left(\frac{2}{J}\right)^{\frac{1}{2}}, \left(2c_0\delta_0^2\right)^{\frac{1}{2}}, \left(2c_1e_0\delta_1^2\right)^{\frac{1}{2}}, \left(2c_2e_0\delta_2^2\right)^{\frac{1}{2}}\right\}$ and $\phi = \delta_0\left(\bar{\gamma}_0 + \frac{\bar{\gamma}_0^2}{4}\right) + e_0\delta_1\left(\bar{\gamma}_1 + \frac{\bar{\gamma}_1^2}{4}\right) + e_0\delta_2\left(\bar{\gamma}_2 + \frac{\bar{\gamma}_2^2}{4}\right)$, respectively.

Thus, the time derivative of the candidate Lyapunov function (58) can be further written as the following form:

$$\dot{V}_2 \leq -\left(\delta - \frac{\phi}{V_2^{\frac{1}{2}}}\right)V_2^{\frac{1}{2}}. \tag{59}$$

From (59), if $\delta - \frac{\phi}{\left(\frac{1}{2}s^T J^* s\right)^{\frac{1}{2}}} > 0$, then $\delta - \frac{\phi}{V_2^{\frac{1}{2}}} > 0$ is obtained such that the finite-time reachability of sliding manifold can be guaranteed by using Lemma 2. Hence, the region $\|s\| \leq \Delta_s$ can be reached in finite time, where Δ_s is defined as

$$\Delta_s = \sqrt{\frac{2}{J}}\frac{\phi}{\delta}. \tag{60}$$

Moreover, for any sliding variable s_j in the region Δ_s, we have $|s_j| \leq \Delta_s$, $j = 1, 2, 3$. Then, the sliding mode manifold defined in (20) can be written as follows:

$$\dot{q}_{vj} + \alpha q_{vj} + \beta sig\left(q_{vj}\right)^r = \eta_j, \qquad |\eta_j| \leq \Delta_s \tag{61}$$

Then, equation (61) can be written as the following two forms:

$$\dot{q}_{vj} + \left(\alpha - \frac{\eta_j}{q_{vj}}\right) q_{vj} + \beta sig\left(q_{vj}\right)^r = 0 \tag{62a}$$

$$\dot{q}_{vj} + \alpha q_{vj} + \left(\beta - \frac{\eta_j}{sig\left(q_{vj}\right)^r}\right) sig\left(q_{vj}\right)^r = 0. \tag{62b}$$

From euqation (62a), if $\alpha - \frac{\eta_j}{q_{vj}} > 0$, a similar structure to the proposed sliding mode manifold is kept. Therefore, the finite-time attitude stabilization is guaranteed by using Lemma 4. Furthermore, the attitude q_{vj} will converge to the region

$$|q_{vj}| \leq \frac{|\eta_j|}{\alpha} \leq \frac{\Delta_s}{\alpha} \tag{63a}$$

in finite time. By similar analysis for (62b) and Lemma 4, the attitude $q_{v,j}$ will also converge to the region

$$|q_{vj}| \leq \left(\frac{|\eta_j|}{\beta}\right)^{\frac{1}{r}} \leq \left(\frac{\Delta_s}{\beta}\right)^{\frac{1}{r}} \tag{63b}$$

in finite time. Finally, the attitude q_{vj} will converge to the region

$$|q_{vj}| \leq \min\left\{\frac{\Delta_s}{\alpha}, \left(\frac{\Delta_s}{\beta}\right)^{\frac{1}{r}}\right\} \tag{64}$$

in finite time. Moreover, from (61), $\dot{q}_{vj}$ will converge to the region

$$|\dot{q}_{vj}| \leq |\eta_j| + \alpha\left|q_{vj}\right| + \beta\left|q_{vj}\right|^r \leq 3\Delta_s \tag{65}$$

in finite time.

It should be noted that $||R(q_v) + q_0 I_3|| = 1$. From (2), it can be obtained that $||\omega|| = 2||\dot{q}_v||$, which further indicates that $||\omega||_\infty \leq 2\sqrt{3}||\dot{q}_v||_\infty$. On the other hand, since $\dot{q}_v$ will converge to the region $|\dot{q}_{vj}| \leq 3\Delta_s$ $(j = 1, 2, 3)$ in finite time, it is clear that $||\dot{q}_v||_\infty \leq 3\Delta_s$ will be satisfied in finite time. Therefore, it can be shown that the angular velocity will converge the region $|\omega_j| \leq 6\sqrt{3}\Delta_s$ in finite time. This completes the proof. □

APPENDIX D

Proof of Theorem 3. Consider the following Lyapunov function candidate V_3:

$$V_3 = \frac{1}{2}s^T J^* s + \frac{1}{2c_0}\left(\hat{\theta}_0 - \bar{\theta}_0\right)^2 + \frac{e_0}{2c_1}\left(\hat{\theta}_1 - \bar{\theta}_1\right)^2 + \frac{e_0}{2c_2}\left(\hat{\theta}_2 - \bar{\theta}_2\right)^2 + \frac{e_0}{2c_3}\left(\hat{\theta}_3^{-1} - \bar{\theta}_1^{-1}\right)^2. \tag{66}$$

With the application of controller (42) and Property 2, the time derivative of V_3 results in

$$\begin{aligned}\dot{V}_3 \leq & -k\|s\| + (1 - e_0\kappa)\|P\|\|u_{nom}\|\|Ps\| + f_0\|D\|\|Ps\| + \theta_0\Omega\|s\| - e_0\kappa\zeta\hat{\theta}_3\left(\hat{\theta}_1\|D\| + \hat{\theta}_2\|P\|\|u_{nom}\|\right)\|Ps\| \\ & - \hat{\theta}_0\Omega\|s\| + \frac{1}{c_0}(\hat{\theta}_0 - \bar{\theta}_0)\dot{\hat{\theta}}_0 + \frac{e_0}{c_1}(\hat{\theta}_1 - \bar{\theta}_1)\dot{\hat{\theta}}_1 + \frac{e_0}{c_2}(\hat{\theta}_2 - \bar{\theta}_2)\dot{\hat{\theta}}_2 - \frac{e_0}{c_3\hat{\theta}_3^2}(\hat{\theta}_3^{-1} - \bar{\theta}_3^{-1})\dot{\hat{\theta}}_3.\end{aligned} \tag{67}$$

To prove the stability of the closed-loop system with saturated adaptive finite-time FTC law, two cases need to be considered based on the defined projection operator.

Case 1: $\hat{\theta}_3 > 1$ or $\hat{\theta}_3 = 1$ and $\bullet \geq 0$. In this case, it can be found from (44d) that

$$\dot{\hat{\theta}}_3 = c_3\zeta\hat{\theta}_3^3\left[\left(\hat{\theta}_1\|D\| + \hat{\theta}_2\|P\|\|u_{nom}\|\right)\|Ps\| - \delta_3\hat{\theta}_3\right]. \tag{68}$$

Then, according to the adaptive laws defined in (44a)-(44c) and (68), it follows from expression (67) that

$$\begin{aligned}\dot{V}_3 \leq & -k\|s\| + (\theta_0 - \bar{\theta}_0)\Phi\|s\| + (f_0 - e_0\bar{\theta}_1)\|D\|\|Ps\| + (1 - e_0\kappa - e_0\bar{\theta}_2)\|P\|\|u_{nom}\|\|Ps\| \\ & + (\bar{\theta}_3^{-1} - \kappa)e_0\zeta\hat{\theta}_3\left(\hat{\theta}_1\|D\| + \hat{\theta}_2\|P\|\|u_{nom}\|\right)\|Ps\| - \delta_0(\hat{\theta}_0 - \bar{\theta}_0)\hat{\theta}_0 - e_0\delta_1(\hat{\theta}_1 - \bar{\theta}_1)\hat{\theta}_1 \\ & - e_0\delta_2(\hat{\theta}_2 - \bar{\theta}_2)\hat{\theta}_2 - e_0\zeta\delta_3(\bar{\theta}_3^{-1}\hat{\theta}_3 - 1)\hat{\theta}_3. \end{aligned} \tag{69}$$

Here, it should be noted that $\hat{\theta}_1(t) \geq 0$ and $\hat{\theta}_2(t) \geq 0$. Considering the following inequalities:

$$-(\hat{\theta}_i - \bar{\theta}_i)\hat{\theta}_i \leq -\left(\hat{\theta}_i - \frac{\bar{\theta}_i}{2}\right)^2 + \frac{\bar{\theta}_i^2}{4}, \tag{70}$$

$$-(\bar{\theta}_3^{-1}\hat{\theta}_3 - 1)\hat{\theta}_3 \leq -\bar{\theta}_3^{-1}\left[\left(\hat{\theta}_3 - \frac{\bar{\theta}_3}{2}\right)^2 + \frac{\bar{\theta}_3^2}{4}\right], \tag{71}$$

the Lyapunov function candidate can be further written as

$$\begin{aligned}\dot{V}_3 \leq & -k\|s\| - \delta_0\left|\hat{\theta}_0 - \bar{\theta}_0\right| - e_0\delta_1\left|\hat{\theta}_1 - \bar{\theta}_1\right| - e_0\delta_2\left|\hat{\theta}_2 - \bar{\theta}_2\right| - e_0\zeta\delta_3\left|\hat{\theta}_3^{-1} - \bar{\theta}_3^{-1}\right| + \delta_0\left(\left|\hat{\theta}_0 - \bar{\theta}_0\right| + \frac{\bar{\theta}_0^2}{4}\right) \\ & + e_0\delta_1\left(\left|\hat{\theta}_1 - \bar{\theta}_1\right| + \frac{\bar{\theta}_1^2}{4}\right) + e_0\delta_2\left(\left|\hat{\theta}_2 - \bar{\theta}_2\right| + \frac{\bar{\theta}_2^2}{4}\right) + e_0\zeta\delta_3\left(\left|\hat{\theta}_3^{-1} - \bar{\theta}_3^{-1}\right| + \frac{\bar{\theta}_3}{4}\right).\end{aligned}$$

Invoking the fact $\hat{\theta}_3 \geq 1$, Lemma 1, and Lemma 6, the following inequalities are held:

$$\dot{V}_3 \leq -\eta_1 V_3^{\frac{1}{2}} + \varphi_1, \tag{72}$$

where η_1 and φ_1 are defined as $\eta_1 = \min\left\{k\left(\frac{2}{\overline{J}}\right)^{\frac{1}{2}}, \left(2c_0\delta_0^2\right)^{\frac{1}{2}}, \left(2c_1e_0\delta_1^2\right)^{\frac{1}{2}}, \left(2c_2e_0\delta_2^2\right)^{\frac{1}{2}}, \left(2c_3e_0\zeta^2\delta_3^2\right)^{\frac{1}{2}}\right\}$, and $\varphi_1 = \delta_0\left(\bar{\theta}_0 + \frac{\bar{\theta}_0^2}{4}\right) + e_0\delta_1\left(\bar{\theta}_1 + \frac{\bar{\theta}_1^2}{4}\right) + e_0\delta_2\left(\bar{\theta}_2 + \frac{\bar{\theta}_2^2}{4}\right) + e_0\zeta\delta_3\left(1 + \frac{\bar{\theta}_3}{4}\right)$.

Comparing the inequalities (72) with (58), it is clear that two inequalities have a similar structure. Following the same lines as in the proof of Theorem 2, it can be shown that the sliding mode manifold will converge to the neighborhood of $s = 0$ as

$$\|s\| \leq \Delta_{sat1}, \tag{73}$$

in finite time, where $\Delta_{sat1} = \sqrt{\frac{2}{\underline{J}}\frac{\varphi_1}{\eta_1}}$. Furthermore, the spacecraft attitude q_{vj} and angular velocity ω_j will converge to the regions

$$|q_{vj}| \leq \min\left\{\frac{\Delta_{sat1}}{\alpha}, \left(\frac{\Delta_{sat1}}{\beta}\right)^{\frac{1}{r}}\right\}, \tag{74}$$

$$|\omega_j| \leq 6\sqrt{3}\Delta_{sat1}, \tag{75}$$

in finite time, respectively.

Case 2: $\hat{\theta}_3 = 1$ and $\bullet < 0$. In this case, there does not exist input saturation and $\hat{\theta}_3 = 1$.

Substituting $\hat{\theta}_3 = 1$ into the control law (42), the saturated adaptive finite-time FTC law is obtained as

$$u_c = -D^T P\left[u_{nom} + \zeta\left(\hat{\gamma}_1\|D\| + \hat{\gamma}_2\|P\|\|u_{nom}\|\right)\frac{s}{\|Ps\|}\right],$$

which is similar to the unsaturated adaptive finite-time FTC law as given in (32) except for the gain constant ζ. Following the same lines as in the proof of Theorem 2, it can also be shown that the sliding variable s, the spacecraft attitude q_{vj}, and angular velocity ω_j $(j = 1, 2, 3)$ will converge to the regions

$$\|s\| \leq \Delta_{sat2}, \tag{76}$$

$$|q_{vj}| \leq \min\left\{\frac{\Delta_{sat2}}{\alpha}, \left(\frac{\Delta_{sat2}}{\beta}\right)^{\frac{1}{r}}\right\}, \tag{77}$$

$$|\omega_j| \leq 6\sqrt{3}\Delta_{sat2}, \tag{78}$$

in finite time, where $\Delta_{sat2} = \sqrt{\frac{2}{J}\frac{\varphi_2}{\eta_2}}$ with $\eta_2 = \min\left\{k\left(\frac{2}{J}\right)^{\frac{1}{2}}, \left(2c_0\delta_0^2\right)^{\frac{1}{2}}, \left(2c_1e_0\delta_1^2\right)^{\frac{1}{2}}, \left(2c_2e_0\delta_2^2\right)^{\frac{1}{2}}\right\}$, and $\varphi_2 = \delta_0\left(\bar{\theta}_0 + \frac{\bar{\theta}_0^2}{4}\right) + e_0\delta_1\left(\bar{\theta}_1 + \frac{\bar{\theta}_1^2}{4}\right) + e_0\delta_2\left(\bar{\theta}_2 + \frac{\bar{\theta}_2^2}{4}\right)$.

Finally, summarizing Case 1 and Case 2, it can be concluded that the sliding variable s, the spacecraft attitude q_{vj}, and angular velocity ω_j $(j = 1, 2, 3)$ will converge to the regions

$$\|s\| \leq \Delta_{sat}, \tag{79}$$

$$|q_{vj}| \leq \min\left\{\frac{\Delta_{sat}}{\alpha}, \left(\frac{\Delta_{sat}}{\beta}\right)^{\frac{1}{r}}\right\}, \tag{80}$$

$$|\omega_j| \leq 6\sqrt{3}\Delta_{sat}, \tag{81}$$

in finite time, where $\Delta_{sat} = \max\{\Delta_{sat1}, \Delta_{sat2}\} = \sqrt{\frac{2}{J}\frac{\varphi}{\eta}}$ with $\eta = \min\{\eta_1, \eta_2\} = \min\left\{k\left(\frac{2}{J}\right)^{\frac{1}{2}}, \left(2c_0\delta_0^2\right)^{\frac{1}{2}}, \left(2c_1e_0\delta_1^2\right)^{\frac{1}{2}}, \left(2c_2e_0\delta_2^2\right)^{\frac{1}{2}}, \left(2c_3e_0\zeta^2\delta_3^2\right)^{\frac{1}{2}}\right\}$, and $\varphi = \max\{\varphi_1, \varphi_2\} = \delta_0\left(\bar{\theta}_0 + \frac{\bar{\theta}_0^2}{4}\right) + e_0\delta_1\left(\bar{\theta}_1 + \frac{\bar{\theta}_1^2}{4}\right) + e_0\delta_2\left(\bar{\theta}_2 + \frac{\bar{\theta}_2^2}{4}\right) + e_0\zeta\delta_3\left(1 + \frac{\bar{\theta}_3}{4}\right)$. This completes the proof. □

REFERENCES

[1] Blanke, M., Izadi-Zamanabadi, R., Bosh, S. A., and Lunau, C. P., "Fault-tolerant control systems - a holistic view," *Control Engineering Practice*, vol. 5, no. 5, pp. 693–702, May 1997.

[2] Patton, R. J., "Fault-tolerant control systems: the 1997 situation," in *Proceedings of the IFAC symposium on fault detection supervision and safety for technical processes*, vol. 3, 1997, pp. 1033–1054.

[3] Zhang, Y. M., and Jiang, J., "Bibliographical review on reconfigurable fault-tolerant control systems," *Annual Reviews in Control*, vol. 32, no. 2, pp. 229–252, Dec. 2008.

[4] Zhang, X. D., Parisini, T., and Polycarpou, M. M., "Adaptive fault-tolerant control of nonlinear uncertain systems: an information-based diagnostic approach," *IEEE Transactions on Automatic Control*, vol. 49, no. 8, pp. 1259–1274, Aug. 2004.

[5] Benosman, M., and Lum, K. Y., "Passive actuators' fault-tolerant control for affine nonlinear nystems," *IEEE Transactions on Control Systems Technology*, vol. 18, no. 1, pp. 152–163, Jan. 2010.

[6] Tafazoli, S., and Khorasani, K., "Nonlinear control and stability analysis of spacecraft attitude recovery," *IEEE Transactions on Aerospace and Electronic Systems*, vol. 42, no. 3, pp. 825–845, Jul. 2006.

[7] Cai, W. C., Liao, X. H., and Song, Y. D., "Indirect robust adaptive fault-tolerant control for attitude tracking of spacecraft," *Journal of Guidance, Control, and Dynamics*, vol. 31, no. 5, pp. 1456–1463, Sep.-Oct. 2008.

[8] Hu, Q. L., Xiao, B., and Zhang, Y. M., "Fault-tolerant attitude control for spacecraft under loss of actuator effectiveness," *Journal of Guidance, Control, and Dynamics*, vol. 34, no. 3, pp. 927–932, May-Jun. 2011.

[9] Xiao, B., Hu, Q. L., and Shi, P., "Attitude stabilization of spacecrafts under actuator saturation and partial loss of control effectiveness," *IEEE Transactions on Control Systems Technology*, vol. 21, no. 6, pp. 2251–2263, Nov. 2013.

[10] Bustan, D., Sani, S. K. H., and Pariz, N., "Adaptive fault-tolerant spacecraft attitude control design with transient response control," *IEEE/ASME Transactions on Mechatronics*, vol. 19, no. 4, pp. 1404–1411, Aug. 2014.

[11] Verbin, D., and Lappas, V. J., "Rapid rotational maneuvering of rigid satellites with hybrid actuators configuration," *Journal of Guidance, Control, and Dynamics*, vol. 36, no. 2, pp. 532–547, Mar.-Apr. 2013.

[12] Bhat S. P., and Bernstein, D. S., "Finite-time stability of continuous autonomous systems," *SIAM Journal on Control and Optimization*, vol. 38, no. 3, pp. 751–766, 2000.

[13] Du, H. B, Li, S. H., and Qian, C. J., "Finite-time attitude tracking control of spacecraft with application to attitude synchronization," *IEEE Transactions on Automatic Control*, vol. 56, no. 11, pp. 2711–2717, Nov. 2011.

[14] Amato, F., Ariola, M., and Dorato, P., "Finite-time control of linear systems subject to parametric uncertainties and disturbances," *Automatica*, vol. 37, no. 9, pp. 1459–1463, Sep. 2001.

[15] Zhu, Z., Xia, Y. Q., and Fu, M. Y., "Attitude stabilization of rigid spacecraft with finite-time convergence," *International Journal of Robust and Nonlinear Control*, vol. 21, no. 6, pp. 686–702, Apr. 2011.

[16] Zou, A. M., and Kumar, K. D., "Distributed attitude coordination control for spacecraft formation flying," *IEEE Transactions on Aerospace and Electronic Systems*, vol. 48, no. 2, pp. 1329–1346, Apr. 2012.

[17] Su, Y., and Zheng, C., "Simple nonlinear proportional-derivative control for global finite-time stabilization of spacecraft," *Journal Guidance, Control, and Dynamics*, vol. 38, no. 1, pp. 173–178, Jan. 2015.

[18] Xiao, B., Hu, Q., Wang, D., and Poh, E. K., "Attitude tracking control of rigid spacecraft with actuator misalignment and fault," *IEEE Transactions on Control Systems Technology*, vol. 6, no. 21, pp. 2360–2366, Nov. 2013.

[19] Zhang, Y., and Jiang, J., "Fault tolerant control system design with explicit consideration of performance degradation," *IEEE Transactions on Aerospace and Electronic Systems*, vol. 39, no. 3, pp. 838–848, Jul. 2003.

[20] Boskovic J. D., and Mehra, R. K., "A decentralized fault-tolerant control system for accommodation of failures in higher-order flight control actuators," *IEEE Transactions on Control Systems Technology*, vol. 18, no. 5, pp. 1103–1115, Sep. 2010.

[21] Gayaka, S., and Yao, B., "Adaptive robust actuator fault-tolerant control in presence of input saturation," in *Proceeding of American Control Conference*, San Francisco, CA, Jun.-Jul. 2011, pp. 3766–3771.

[22] Xiao, B., Hu, Q., Zhang, Y., and Huo, X., "Fault-tolerant tracking control of spacecraft with attitude-only measurement under actuator failures," *Journal of Guidance, Control, and Dynamics*, vol. 37, no. 3, pp. 838–849, May-Jun. 2014.

[23] Tsiotras, P., and Luo, J., "Control of underactuated spacecraft with bounded inputs," *Automatica*, vol. 36, no. 8, pp. 1153–1169, Aug. 2000.

[24] Boskovic, J. D., Li, S., and Mehra, R. K., "Robust adaptive variable structure control of spacecraft under control input saturation," *Journal Guidance, Control, and Dynamics*, vol. 24, no. 1, pp. 14–22, Jul.-Aug. 2001.

[25] Lovera, M., and Astolfi, A., "Spacecraft attitude control using magnetic actuators," *Automatica*, vol. 40, no. 8, pp. 1405–1414, Aug. 2004.

[26] Zhu, Z., Xia, Y. Q., and Fu, M. Y., "Adaptive sliding mode control for attitude stabilization with actuator saturation," *IEEE Transactions on Industrial Electronics*, vol. 58, no. 10, pp. 4898–4907, Oct. 2011.

[27] Sidi, M. J., *Spacecraft Dynamics and Control*. Cambridge, U.K.: Cambridge University Press, 1997.

[28] Wie, B., *Space Vehicle Dynamics and Control*. AIAA, Reston, VA: AIAA Education Series, 2008.

[29] Alwi, H., and Edwards, C., "Fault tolerant control using sliding modes with on-line control allocation," *Automatica*, vol. 44, no. 7, pp. 1859–1866, Jul. 2008.

[30] Zhang, Y., Rabbath, C. A., and Su, C.-Y., "Reconfigurable control allocation applied to an aircraft benchmark model," in *Proceeding of American Control Conference*, Seattle, WA, 2008, pp. 1052–1057.

[31] Benosman, M., and Lum, K. Y., "Online references reshaping and control reallocation for nonlinear fault tolerant control," *IEEE Transactions on Control Systems Technology*, vol. 17, no. 2, pp. 366–379, Mar. 2009.

[32] Hamayun, M. T., Edwards, C., and Alwi, H., "Design and analysis of an integral sliding mode fault-tolerant control scheme," *IEEE Transactions on Automatic Control*, vol. 57, no. 7, pp. 1783–1789, Jul. 2012.

[33] Page, A. B., and Steinberg, M. L., "Effects of control allocation algorithms on a nonlinear adaptive design," in *AIAA Guidance, Navigation, and Control Conference*. AIAA, Reston, VA, Aug. 1999.

[34] ——, "A closed-loop comparison of control allocation methods," in *AIAA Guidance, Navigation, and Control Conference*. AIAA, Reston, VA, Aug. 2000.

[35] Zhang, Y., and Chen, Z., "A closed-loop control allocation method for satellite precision pointing," in *IEEE International Conference on Industrial Informatics*. IEEE Publications, 2012, pp. 1108–1112.

[36] Hu, Q., Li, B., and Zhang, Y., "Nonlinear proportional-derivative control incorporating closed-loop control allocation for spacecraft," *Journal of Guidance, Control, and Dynamics*, vol. 37, no. 3, pp. 799–812, May-Jun. 2014.

[37] Jin, J., Ko, S., and Ryoo, C. K., "Fault tolerant control for satellites with four reaction wheels," *Control Engineering Practice*, vol. 16, no. 10, pp. 1250–1258, Oct. 2008.

[38] Murugesan, S., and Goel, P. S., "Fault-tolerant spacecraft attitude control system," *Sadhana-Academy Proceedings in Engineering Sciences*, vol. 11, no. 1-2, pp. 233–261, 1987.

[39] Godard, "Fault tolerant control of spacecraft," Ph.D. dissertation, Ryerson University, Toronto, Ontario, Canada, 2010.

[40] Blanke, M., Kinnaert, M., Lunze, J., and Staroswiecki, M., *Diagnosis and Fault-Tolerant Control*, 2nd ed. Berlin, Germany: Springer, 2006.

[41] Costic, B. T., Dawson, D. M., Queiroz, M. S., and Kapila, V., "Quaternion-based adaptive attitude tracking controller without velocity measurements," *Journal of Guidance, Control, and Dynamics*, vol. 24, no. 6, pp. 1214–1222, Nov.-Dec. 2001.

[42] Wu, B. L., Wang, D. W., and Poh, E. K., "Decentralized robust adaptive control for attitude synchronization under directed communication topology," *Journal of Guidance, Control, and Dynamics*, vol. 34, no. 3, pp. 1276–1282, Jul.-Aug. 2011.

[43] Zhao, D. Y., Li, S. Y., and Zhu, Q. M., "A new TSMC prototype robust nonlinear task space control of a 6 DOF parallel robotic manipulator," *International Journal of Control, Automation and Systems*, vol. 8, no. 6, pp. 1189–1197, Dec. 2010.

[44] Yu, S. H., Yu, X. H., Shirinzadeh, B., and Man, Z. H., "Continuous finite-time control for robotic manipulators with terminal sliding mode," *Automatica*, vol. 41, no. 11, pp. 1957–1964, Nov. 2005.

[45] Huang, X., Lin, W., and Yang, B., "Global finite-time stabilization of a class of uncertain nonlinear systems," *Automatica*, vol. 41, no. 5, pp. 881–888, May 2005.

[46] Shuster, M. D., "A survey of attitude representations," *Journal of the Astronautical Sciences*, vol. 41, no. 4, pp. 439–517, Oct.-Dec. 1993.

[47] Du H., and Li, S., "Finite-time attitude stabilization for a spacecraft using homogeneous method," *Journal of Guidance, Control, and Dynamics*, vol. 35, no. 3, pp. 740–748, May-Jun. 2012.

[48] Shen, Q., Wang, D. W., Zhu, S. Q., and Poh, E. K., "Integral-type sliding mode fault-tolerant control for attitude stabilization of spacecraft," *IEEE Transactions on Control Systems Technology*, 2014, to be published. [Online]. Available: 10.1109/TCST.2014.2354260

[49] Hu, Q. L., Ma, G. F., and Xie, L. H., "Robust and adaptive variable structure output feedback control of uncertain systems with input nonlinearity," *Automatica*, vol. 44, no. 2, pp. 552–559, Feb. 2008.

[50] Hu, Q. L., "Robust adaptive sliding mode attitude maneuvering and vibration damping of three-axis-stabilized flexible spacecraft with actuator saturation limits," *Nonlinear Dynamics*, vol. 55, no. 4, pp. 301–321, Mar. 2009.

[51] Yu, X. H., and Kaynak, O., "Sliding-mode control with soft computing: a survey," *IEEE Transactions on Industrial Electronics*, vol. 56, no. 9, pp. 3275–3285, Sep. 2009.

[52] Baldi, P., Castaldi, P., Mimmo, N., and Simani, S., "A new aerodynamic decoupled frequential FDIR methodology for satellite actuator faults," *International Journal of Adaptive Control and Signal Processing*, vol. 28, no. 9, pp. 812–832, Sep. 2014.

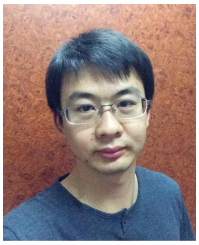

Qiang Shen (S'12) received the B.E. degree from Northwestern Polytechnical University, Xian, P.R. China, in 2010. He is currently working towards the Ph.D. degree at Nanyang Technological University, Singapore. His research interests include fault-tolerant control and applications, spacecraft attitude control and control allocation.

Danwei Wang (S'88-M'89-SM'04) received his Ph.D and MSE degrees from the University of Michigan, Ann Arbor in 1989 and 1984, respectively. He received his B.E degree from the South China University of Technology, China in 1982. He is professor in the School of Electrical and Electronic Engineering, Nanyang Technological University, Singapore. He is director of the Centre for E-City and director of the STE-NTU Corp Lab, NTU. He has served as general chairman, technical chairman and various positions in international conferences. He has served as an associate editor of Conference Editorial Board, IEEE Control Systems Society. He is an associate editor of International Journal of Humanoid Robotics and invited guest editor of various international journals. He was a recipient of Alexander von Humboldt fellowship, Germany. He has published widely in the areas of iterative learning control, repetitive control, fault diagnosis and failure prognosis, satellite formation dynamics and control, as well as manipulator/mobile robot dynamics, path planning, and control.

Senqiang Zhu (S'11-M'13) received his B.S. and M.S. degrees in mechanical engineering from Tsinghua University, Beijing, China in 2005 and 2007, respectively, and his Ph.D. degree in electrical and electronic engineering from Nanyang Technological University, Singapore, in 2014. He is currently a Reseach Fellow in the School of electrical and electronic engineering, Nanyang Technological University. His research interests include UAV control, satellite attitude control, and multi-agent cooperation.

Eng Kee Poh obtained his B. Eng (Elec. Eng), First Class Honours, in 1986 from the National University of Singapore. From 1986 to 1989, he worked as a research engineer with DSO National Laboratories specializing in autopilot design and signal processing. Subsequently, he received his M. Sc (Elec. Eng.: Systems) and PhD (Elec. Eng.: Systems) from the University of Michigan in 1990 and 1993 respectively. Dr. Poh is presently a distinguished member of technical staff (DMTS) cum Laboratory Head (Guidance, Navigation and Control) in DSO National Laboratories, He holds a concurrent position as Associate Professor (Adjunct) at the Nanyang Technological University. His current interests are in navigation technology, control theory and signal processing algorithms.

Fig. 1. Spacecraft attitude response under BFT-FTC scheme and PDC scheme. (a) BFT-FTC; (b) PDC

Fig. 2. Spacecraft angular velocity response under BFT-FTC scheme and PDC scheme. (a) BFT-FTC; (b) PDC

Fig. 3. Commanded control torque under BFT-FTC scheme and PDC scheme. (a) BFT-FTC; (b) PDC

Fig. 4. Spacecraft attitude under AFT-FTC scheme and IRA-FTC scheme. (a) AFT-FTC; (b) IRA-FTC

Fig. 5. Spacecraft angular velocity response under AFT-FTC scheme and IRA-FTC scheme. (a) AFT-FTC; (b) IRA-FTC

Fig. 6. Commanded control torque under AFT-FTC scheme and IRA-FTC scheme. (a) AFT-FTC; (b) IRA-FTC

Fig. 7. Time response of adaptive parameters $\hat{\gamma}_0(t)$, $\hat{\gamma}_1(t)$, and $\hat{\gamma}_2(t)$ under AFT-FTC scheme.

Fig. 8. Spacecraft attitude under SAFT-FTC scheme and SIRA-FTC scheme. (a)SAFT-FTC; (b) SIRA-FTC

Fig. 9. Spacecraft angular velocity response under SAFT-FTC scheme and SIRA-FTC scheme. (a)SAFT-FTC; (b) SIRA-FTC

Fig. 10. Commanded control torque under SAFT-FTC scheme and SIRA-FTC scheme. (a)SAFT-FTC; (b) SIRA-FTC

Fig. 11. Time response of adaptive parameters $\hat{\theta}_0(t)$, $\hat{\theta}_1(t)$, $\hat{\theta}_2(t)$, and $\hat{\theta}_3(t)$ under SAFT-FTC scheme.